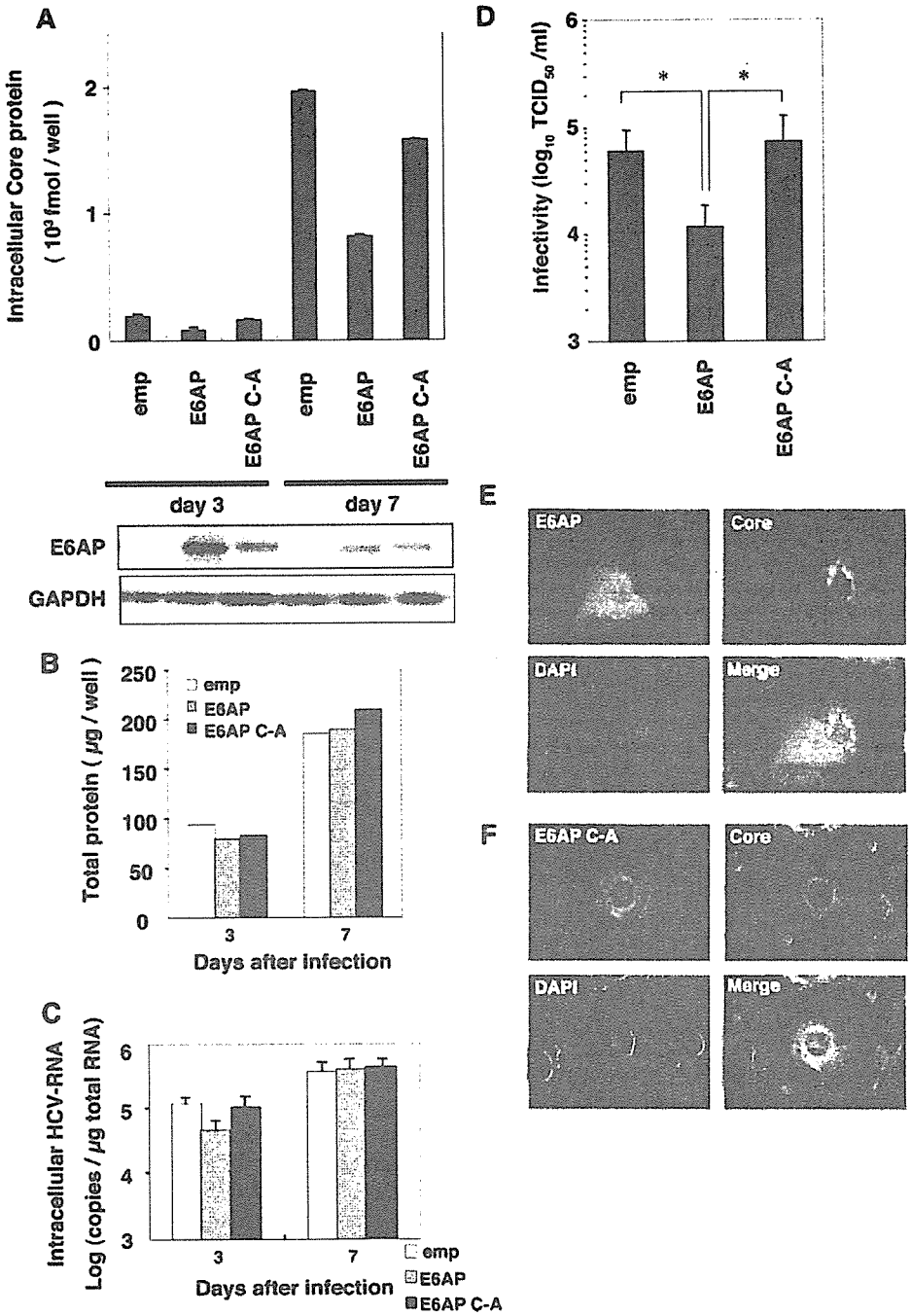

FIG. 9. Exogenous expression of E6AP reduces intracellular HCV core protein levels and supernatant infectivity titers in HCV-infected Huh-7 cells. Naïve Huh-7 cells were seeded as described in Materials and Methods; inoculated with 2.5 ml of the inoculum including infectious HCV JFH1 (6.5×10^3 $TCID_{50}$/ml); and transfected with 6 μg of empty plasmid, pCAG-HA-E6AP, or pCAG-HA-E6AP C-A. The culture supernatant and the cells were collected at days 3 and 7 postinfection. (A) Intracellular HCV core protein levels. (B) Levels of total protein. (C) Levels of intracellular HCV RNA in HCV-infected Huh-7 cells. Data represent the averages of three experiments with error bars. (D) Supernatant infectivity titers. At day 7 postinfection, culture supernatants were collected and assayed for $TCID_{50}$ determinations. The difference between empty vector and E6AP or between E6AP and E6AP C-A was significant (*, $P < 0.05$, Student's t test). (E and F) HCV JFH1-infected Huh-7 cells were transfected with either MEF-E6AP plasmid or MEF-E6AP C-A plasmid, grown on coverslips, fixed, and processed for double-label immunofluorescence for HCV core and MEF-E6AP (E) or MEF-E6AP C-A (F). Anticore MAb (2H9) and anti-FLAG PAb were used as primary antibodies. Nuclei were visualized by staining the cells with DAPI. All the samples were examined with a BZ-8000 microscope. Representative images of individual cells are shown with merge images. emp, empty vector.

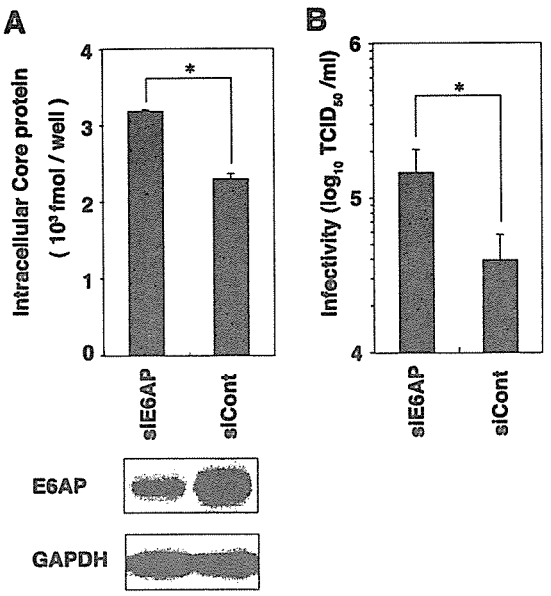

FIG. 10. E6AP silencing leads to an increase in the level of intracellular HCV core protein and supernatant infectivity titer in HCV-infected Huh-7 cells. (A) HCV JFH1-infected cells were replated in a six-well plate at 3×10^5 cells/well and transfected with 40 pmol of E6AP siRNA or control siRNA. The culture medium was changed at 24 h after transfection. The cells were harvested at day 2 after transfection, and the intracellular core protein levels were quantitated using the HCV core antigen ELISA. Equivalent amounts of the whole-cell lysates were separated by SDS-PAGE and analyzed by immunoblotting with anti-E6AP MAb or anti-GAPDH MAb. (B) Culture supernatants were collected at day 2 after transfection and assayed for $TCID_{50}$ determinations. For both panels, the difference between E6AP siRNA and control siRNA was significant (*, $P < 0.05$, Student's t test).

in a ubiquitin-independent, ATP-independent, and 20S proteasome-dependent pathway (27). There have been reports that several cellular factors, such as p53 (2), p73 (2), and RPN4 (18), are degraded through two alternative pathways, the ubiquitin-dependent 26S proteasome-dependent pathway and the ubiquitin-independent 20S proteasome-dependent pathway. Here we provide evidence that E6AP mediates ubiquitylation of HCV core protein. Still unclear is whether the PA28γ-dependent pathway requires polyubiquitylation of HCV core protein. HCV core protein is predominantly localized in the cytoplasm, especially at the endoplasmic reticulum membrane, on the surface of lipid droplets, and on mitochondria and mitochondrion-associated membranes (51). In HCV JFH1-infected cells, HCV core was found to localize in the cytoplasm and frequently to accumulate in the perinuclear region and the lipid droplets (44). Our results indicated that E6AP colocalized with HCV core protein especially in the perinuclear region. PA28γ was found to colocalize with HCV core protein in the nucleus. Functional differences may exist between the E6AP-dependent pathway and the PA28γ-dependent pathway in the stability control of HCV core protein. The functional role of the E6AP-dependent pathway and the PA28γ-dependent pathway remains to be elucidated.

The HCV core-binding region of E6AP was mapped to the region between aa 418 and aa 517. The multicopy maintenance protein 7, Mcm7, interacts with E6AP through a short motif, termed the L2G box (aa 412 to 414), that lies within the E6 binding site of E6AP (23). Our data indicated that the E6 binding region containing the L2G motif is not required for interaction between HCV core protein and E6AP (Fig. 2C, lane M).

We propose here that E6AP may affect the production of HCV particles through controlling the amounts of HCV core protein. This mechanism may contribute to persistent infection. The E6AP binding domain of the core protein resides in the RNA-binding domain and binding domains for many host factors (40). These factors may affect the binding between E6AP and HCV core protein, resulting in control of E6AP-dependent core degradation. Another possibility is that HCV core protein may affect the normal function of E6AP, thereby contributing to pathogenesis. It will be intriguing to investigate whether HCV core protein has any effect on E6AP-dependent degradation of host factors. The other intriguing possibility is that HCV core-E6AP complex may function as an E3 ligase-like E6-E6AP complex to target host factors for proteasomal degradation and contribute to viral pathogenesis.

In conclusion, we have demonstrated that E6AP interacts with HCV core protein in vitro and in vivo and mediates ubiquitin-dependent degradation of the core protein, leading to downregulation of HCV particles. We propose that the E6AP-mediated ubiquitin-proteasome pathway may play a role in affecting the production of HCV particles through controlling the amounts of viral nucleocapsid protein. Identification of the specific E3 ubiquitin ligase may contribute to gaining a better understanding of the biology of the HCV life cycle as well as molecular details of the ubiquitin-dependent degradation of HCV core protein.

ACKNOWLEDGMENTS

We thank D. Bohmann (EMBL) for providing pMT123, K. Miyazono (University of Tokyo) for pcDEF3-6Myc-WWP1, and K. Iwai (Osaka City University) for recombinant baculovirus carrying His 6-mouse E1. Huh-7.5.1 cells and Huh-7 cells were kindly provided by F. V. Chisari (Scripps Research Institute). We also thank P. Zhou (Weill Medical College of Cornell University), S. I. Wells (Cincinnati Children's Hospital Medical Center), and A. W. Hudson (Medical College of Wisconsin) for critical readings of the manuscript; M. Matsuda, S. Yoshizaki, M. Ikeda, and M. Sasaki for technical assistance; Y. Sugiyama and S. Senzui for plasmid construction; and T. Mizoguchi for secretarial work.

This work was supported in part by a grant for Research on Health Sciences focusing on Drug Innovation from the Japan Health Sciences Foundation; by grants-in-aid from the Ministry of Health, Labor and Welfare; by grants-in-aid from the Ministry of Education, Culture, Sports, Science and Technology; and by the program for Promotion of Fundamental Studies in Health Sciences of the National Institute of Biomedical Innovation (NIBIO), Japan. T.I. was supported in part by a grant from Novartis Foundation (Japan) for the Promotion of Science and by the Tokyo Metropolitan University President's Fund, Special Emphasis Research Project of Japan.

REFERENCES

1. **Aizaki, H., Y. Aoki, T. Harada, K. Ishii, T. Suzuki, S. Nagamori, G. Toda, Y. Matsuura, and T. Miyamura.** 1998. Full-length complementary DNA of hepatitis C virus genome from an infectious blood sample. Hepatology **27**: 621–627.
2. **Asher, G., P. Tsvetkov, C. Kahana, and Y. Shaul.** 2005. A mechanism of ubiquitin-independent proteasomal degradation of the tumor suppressors p53 and p73. Genes Dev. **19**:316–321.
3. **Bukh, J., R. H. Purcell, and R. H. Miller.** 1994. Sequence analysis of the core gene of 14 hepatitis C virus genotypes. Proc. Natl. Acad. Sci. USA **91**:8239–8243.

4. **Chen, C., and H. Okayama.** 1987. High-efficiency transformation of mammalian cells by plasmid DNA. Mol. Cell. Biol. **7**:2745–2752.
5. **Choo, Q. L., G. Kuo, A. J. Weiner, L. R. Overby, D. W. Bradley, and M. Houghton.** 1989. Isolation of a cDNA clone derived from a blood-borne non-A, non-B viral hepatitis genome. Science **244**:359–362.
6. **Choo, Q. L., K. H. Richman, J. H. Han, K. Berger, C. Lee, C. Dong, C. Gallegos, D. Coit, R. Medina-Selby, P. J. Barr, et al.** 1991. Genetic organization and diversity of the hepatitis C virus. Proc. Natl. Acad. Sci. USA **88**:2451–2455.
7. **Franck, N., J. Le Seyec, C. Guguen-Guillouzo, and L. Erdtmann.** 2005. Hepatitis C virus NS2 protein is phosphorylated by the protein kinase CK2 and targeted for degradation to the proteasome. J. Virol. **79**:2700–2708.
8. **Gao, L., H. Tu, S. T. Shi, K. J. Lee, M. Asanaka, S. B. Hwang, and M. M. Lai.** 2003. Interaction with a ubiquitin-like protein enhances the ubiquitination and degradation of hepatitis C virus RNA-dependent RNA polymerase. J. Virol. **77**:4149–4159.
9. **Giannini, C., and C. Brechot.** 2003. Hepatitis C virus biology. Cell Death Differ. **10**(Suppl. 1):S27–S38.
10. **Grakoui, A., D. W. McCourt, C. Wychowski, S. M. Feinstone, and C. M. Rice.** 1993. Characterization of the hepatitis C virus-encoded serine proteinase: determination of proteinase-dependent polyprotein cleavage sites. J. Virol. **67**:2832–2843.
11. **Harris, K. F., I. Shoji, E. M. Cooper, S. Kumar, H. Oda, and P. M. Howley.** 1999. Ubiquitin-mediated degradation of active Src tyrosine kinase. Proc. Natl. Acad. Sci. USA **96**:13738–13743.
12. **Hijikata, M., H. Mizushima, T. Akagi, S. Mori, N. Kakiuchi, N. Kato, T. Tanaka, K. Kimura, and K. Shimotohno.** 1993. Two distinct proteinase activities required for the processing of a putative nonstructural precursor protein of hepatitis C virus. J. Virol. **67**:4665–4675.
13. **Huibregtse, J. M., M. Scheffner, S. Beaudenon, and P. M. Howley.** 1995. A family of proteins structurally and functionally related to the E6-AP ubiquitin-protein ligase. Proc. Natl. Acad. Sci. USA **92**:2563–2567.
14. **Huibregtse, J. M., M. Scheffner, and P. M. Howley.** 1993. Cloning and expression of the cDNA for E6-AP, a protein that mediates the interaction of the human papillomavirus E6 oncoprotein with p53. Mol. Cell. Biol. **13**:775–784.
15. **Hussy, P., H. Langen, J. Mous, and H. Jacobsen.** 1996. Hepatitis C virus core protein: carboxy-terminal boundaries of two processed species suggest cleavage by a signal peptide peptidase. Virology **224**:93–104.
16. **Ichimura, T., H. Yamamura, K. Sasamoto, Y. Tominaga, M. Taoka, K. Kakiuchi, T. Shinkawa, N. Takahashi, S. Shimada, and T. Isobe.** 2005. 14-3-3 proteins modulate the expression of epithelial Na^+ channels by phosphorylation-dependent interaction with Nedd4-2 ubiquitin ligase. J. Biol. Chem. **280**:13187–13194.
17. **Iwai, K., K. Yamanaka, T. Kamura, N. Minato, R. C. Conaway, J. W. Conaway, R. D. Klausner, and A. Pause.** 1999. Identification of the von Hippel-Lindau tumor-suppressor protein as part of an active E3 ubiquitin ligase complex. Proc. Natl. Acad. Sci. USA **96**:12436–12441.
18. **Ju, D., and Y. Xie.** 2004. Proteasomal degradation of RPN4 via two distinct mechanisms, ubiquitin-dependent and -independent. J. Biol. Chem. **279**: 23851–23854.
19. **Kao, W. H., S. L. Beaudenon, A. L. Talis, J. M. Huibregtse, and P. M. Howley.** 2000. Human papillomavirus type 16 E6 induces self-ubiquitination of the E6AP ubiquitin-protein ligase. J. Virol. **74**:6408–6417.
20. **Kato, T., M. Miyamoto, A. Furusaka, T. Date, K. Yasui, J. Kato, S. Matsushima, T. Komatsu, and T. Wakita.** 2003. Processing of hepatitis C virus core protein is regulated by its C-terminal sequence. J. Med. Virol. **69**:357–366.
21. **Kishino, T., M. Lalande, and J. Wagstaff.** 1997. UBE3A/E6-AP mutations cause Angelman syndrome. Nat. Genet. **15**:70–73.
22. **Komuro, A., T. Imamura, M. Saitoh, Y. Yoshida, T. Yamori, K. Miyazono, and K. Miyazawa.** 2004. Negative regulation of transforming growth factor-beta (TGF-beta) signaling by WW domain-containing protein 1 (WWP1). Oncogene **23**:6914–6923.
23. **Kuhne, C., and L. Banks.** 1998. E3-ubiquitin ligase/E6-AP links multicopy maintenance protein 7 to the ubiquitination pathway by a novel motif, the L2G box. J. Biol. Chem. **273**:34302–34309.
24. **Kumar, S., A. L. Talis, and P. M. Howley.** 1999. Identification of HHR23A as a substrate for E6-associated protein-mediated ubiquitination. J. Biol. Chem. **274**:18785–18792.
25. **Kunkel, M., M. Lorinczi, R. Rijnbrand, S. M. Lemon, and S. J. Watowich.** 2001. Self-assembly of nucleocapsid-like particles from recombinant hepatitis C virus core protein. J. Virol. **75**:2119–2129.
26. **Kuo, G., Q. L. Choo, H. J. Alter, G. L. Gitnick, A. G. Redeker, R. H. Purcell, T. Miyamura, J. L. Dienstag, M. J. Alter, C. E. Stevens, et al.** 1989. An assay for circulating antibodies to a major etiologic virus of human non-A, non-B hepatitis. Science **244**:362–364.
27. **Li, X., D. M. Lonard, S. Y. Jung, A. Malovannaya, Q. Feng, J. Qin, S. Y. Tsai, M. J. Tsai, and B. W. O'Malley.** 2006. The SRC-3/AIB1 coactivator is degraded in a ubiquitin- and ATP-independent manner by the REGγ proteasome. Cell **124**:381–392.
28. **Lindenbach, B. D., M. J. Evans, A. J. Syder, B. Wolk, T. L. Tellinghuisen, C. C. Liu, T. Maruyama, R. O. Hynes, D. R. Burton, J. A. McKeating, and C. M. Rice.** 2005. Complete replication of hepatitis C virus in cell culture. Science **309**:623–626.
29. **McLauchlan, J., M. K. Lemberg, G. Hope, and B. Martoglio.** 2002. Intramembrane proteolysis promotes trafficking of hepatitis C virus core protein to lipid droplets. EMBO J. **21**:3980–3988.
30. **Moriishi, K., T. Okabayashi, K. Nakai, K. Moriya, K. Koike, S. Murata, T. Chiba, K. Tanaka, R. Suzuki, T. Suzuki, T. Miyamura, and Y. Matsuura.** 2003. Proteasome activator PA28γ-dependent nuclear retention and degradation of hepatitis C virus core protein. J. Virol. **77**:10237–10249.
31. **Moriya, K., H. Fujie, Y. Shintani, H. Yotsuyanagi, T. Tsutsumi, K. Ishibashi, Y. Matsuura, S. Kimura, T. Miyamura, and K. Koike.** 1998. The core protein of hepatitis C virus induces hepatocellular carcinoma in transgenic mice. Nat. Med. **4**:1065–1067.
32. **Moriya, K., H. Yotsuyanagi, Y. Shintani, H. Fujie, K. Ishibashi, Y. Matsuura, T. Miyamura, and K. Koike.** 1997. Hepatitis C virus core protein induces hepatic steatosis in transgenic mice. J. Gen. Virol. **78**:1527–1531.
33. **Natsume, T., Y. Yamauchi, H. Nakayama, T. Shinkawa, M. Yanagida, N. Takahashi, and T. Isobe.** 2002. A direct nanoflow liquid chromatography-tandem mass spectrometry system for interaction proteomics. Anal. Chem. **74**:4725–4733.
34. **Niwa, H., K. Yamamura, and J. Miyazaki.** 1991. Efficient selection for high-expression transfectants with a novel eukaryotic vector. Gene **108**:193–199.
35. **Oda, H., S. Kumar, and P. M. Howley.** 1999. Regulation of the Src family tyrosine kinase Blk through E6AP-mediated ubiquitination. Proc. Natl. Acad. Sci. USA **96**:9557–9562.
36. **Ogino, T., H. Fukuda, S. Imajoh-Ohmi, M. Kohara, and A. Nomoto.** 2004. Membrane binding properties and terminal residues of the mature hepatitis C virus capsid protein in insect cells. J. Virol. **78**:11766–11777.
37. **Okamoto, K., K. Moriishi, T. Miyamura, and Y. Matsuura.** 2004. Intramembrane proteolysis and endoplasmic reticulum retention of hepatitis C virus core protein. J. Virol. **78**:6370–6380.
38. **Owsianka, A. M., and A. H. Patel.** 1999. Hepatitis C virus core protein interacts with a human DEAD box protein DDX3. Virology **257**:330–340.
39. **Pavio, N., D. R. Taylor, and M. M. Lai.** 2002. Detection of a novel unglycosylated form of hepatitis C virus E2 envelope protein that is located in the cytosol and interacts with PKR. J. Virol. **76**:1265–1272.
40. **Polyak, S. J., K. C. Klein, I. Shoji, T. Miyamura, and J. R. Lingappa.** 2006. Assemble and interact: pleiotropic functions of the HCV core protein, p. 89–119. *In* S.-L. Tan (ed.), Hepatitis C viruses: genomes and molecular biology. Horizon Bioscience, Norwich, United Kingdom.
41. **Poynard, T., M. F. Yuen, V. Ratziu, and C. L. Lai.** 2003. Viral hepatitis C. Lancet **362**:2095–2100.
42. **Ravaggi, A., G. Natoli, D. Primi, A. Albertini, M. Levrero, and E. Cariani.** 1994. Intracellular localization of full-length and truncated hepatitis C virus core protein expressed in mammalian cells. J. Hepatol. **20**:833–836.
43. **Ray, R. B., L. M. Lagging, K. Meyer, and R. Ray.** 1996. Hepatitis C virus core protein cooperates with *ras* and transforms primary rat embryo fibroblasts to tumorigenic phenotype. J. Virol. **70**:4438–4443.
44. **Rouille, Y., F. Helle, D. Delgrange, P. Roingeard, C. Voisset, E. Blanchard, S. Belouzard, J. McKeating, A. H. Patel, G. Maertens, T. Wakita, C. Wychowski, and J. Dubuisson.** 2006. Subcellular localization of hepatitis C virus structural proteins in a cell culture system that efficiently replicates the virus. J. Virol. **80**:2832–2841.
45. **Saito, I., T. Miyamura, A. Ohbayashi, H. Harada, T. Katayama, S. Kikuchi, Y. Watanabe, S. Koi, M. Onji, Y. Ohta, et al.** 1990. Hepatitis C virus infection is associated with the development of hepatocellular carcinoma. Proc. Natl. Acad. Sci. USA **87**:6547–6549.
46. **Santolini, E., G. Migliaccio, and N. La Monica.** 1994. Biosynthesis and biochemical properties of the hepatitis C virus core protein. J. Virol. **68**: 3631–3641.
47. **Sato, S., M. Fukasawa, Y. Yamakawa, T. Natsume, T. Suzuki, I. Shoji, H. Aizaki, T. Miyamura, and M. Nishijima.** 2006. Proteomic profiling of lipid droplet proteins in hepatoma cell lines expressing hepatitis C virus core protein. J. Biochem. (Tokyo) **139**:921–930.
48. **Scheffner, M., J. M. Huibregtse, and P. M. Howley.** 1994. Identification of a human ubiquitin-conjugating enzyme that mediates the E6-AP-dependent ubiquitination of p53. Proc. Natl. Acad. Sci. USA **91**:8797–8801.
49. **Scheffner, M., J. M. Huibregtse, R. D. Vierstra, and P. M. Howley.** 1993. The HPV-16 E6 and E6-AP complex functions as a ubiquitin-protein ligase in the ubiquitination of p53. Cell **75**:495–505.
50. **Scheffner, M., U. Nuber, and J. M. Huibregtse.** 1995. Protein ubiquitination involving an E1–E2–E3 enzyme ubiquitin thioester cascade. Nature **373**:81–83.
51. **Suzuki, R., S. Sakamoto, T. Tsutsumi, A. Rikimaru, K. Tanaka, T. Shimoike, K. Moriishi, T. Iwasaki, K. Mizumoto, Y. Matsuura, T. Miyamura, and T. Suzuki.** 2005. Molecular determinants for subcellular localization of hepatitis C virus core protein. J. Virol. **79**:1271–1281.
52. **Suzuki, R., K. Tamura, J. Li, K. Ishii, Y. Matsuura, T. Miyamura, and T. Suzuki.** 2001. Ubiquitin-mediated degradation of hepatitis C virus core pro-

tein is regulated by processing at its carboxyl terminus. Virology **280**:301–309.
53. **Suzuki, T., K. Omata, T. Satoh, T. Miyasaka, C. Arai, M. Maeda, T. Matsuno, and T. Miyamura.** 2005. Quantitative detection of hepatitis C virus (HCV) RNA in saliva and gingival crevicular fluid of HCV-infected patients. J. Clin. Microbiol. **43**:4413–4417.
54. **Takamizawa, A., C. Mori, I. Fuke, S. Manabe, S. Murakami, J. Fujita, E. Onishi, T. Andoh, I. Yoshida, and H. Okayama.** 1991. Structure and organization of the hepatitis C virus genome isolated from human carriers. J. Virol. **65**:1105–1113.
55. **Talis, A. L., J. M. Huibregtse, and P. M. Howley.** 1998. The role of E6AP in the regulation of p53 protein levels in human papillomavirus (HPV)-positive and HPV-negative cells. J. Biol. Chem. **273**:6439–6445.
56. **Wakita, T., T. Pietschmann, T. Kato, T. Date, M. Miyamoto, Z. Zhao, K. Murthy, A. Habermann, H. G. Krausslich, M. Mizokami, R. Bartenschlager, and T. J. Liang.** 2005. Production of infectious hepatitis C virus in tissue culture from a cloned viral genome. Nat. Med. **11**:791–796.
57. **Wertz, I. E., K. M. O'Rourke, Z. Zhang, D. Dornan, D. Arnott, R. J. Deshaies, and V. M. Dixit.** 2004. Human de-etiolated-1 regulates c-Jun by assembling a CUL4A ubiquitin ligase. Science **303**:1371–1374.
58. **Xu, Z., J. Choi, W. Lu, and J. Ou.** 2003. Hepatitis C virus F protein is a short-lived protein associated with the endoplasmic reticulum. J. Virol. **77**: 1578–1583.
59. **Yamaguchi, R., S. Momosaki, G. Gao, C. C. Hsia, M. Kojiro, C. Scudamore, and E. Tabor.** 2004. Truncated hepatitis C virus core protein encoded in hepatocellular carcinomas. Int. J. Mol. Med. **14**:1097–1100.
60. **Yasui, K., T. Wakita, K. Tsukiyama-Kohara, S. I. Funahashi, M. Ichikawa, T. Kajita, D. Moradpour, J. R. Wands, and M. Kohara.** 1998. The native form and maturation process of hepatitis C virus core protein. J. Virol. **72**:6048–6055.
61. **Zhong, J., P. Gastaminza, G. Cheng, S. Kapadia, T. Kato, D. R. Burton, S. F. Wieland, S. L. Uprichard, T. Wakita, and F. V. Chisari.** 2005. Robust hepatitis C virus infection in vitro. Proc. Natl. Acad. Sci. USA **102**:9294–9299.

doi:10.1016/j.jmb.2006.03.020 J. Mol. Biol. (2006) 359, 22–34

JMB

Available online at www.sciencedirect.com

SCIENCE DIRECT®

ELSEVIER

Overexpression of Hepatitis C Virus NS5A Protein Induces Chromosome Instability *via* Mitotic Cell Cycle Dysregulation

Kwan-Hyuck Baek[1,2], Hye-Young Park[1,2], Chang-Mo Kang[3] So-Jung Kim[1], Sook-Jung Jeong[1,2], Eun-Kyung Hong[1] Joong-Won Park[1], Young-Chul Sung[4], Tetsuro Suzuki[5] Chang-Min Kim[1] and Chang-Woo Lee[1,2]*

[1]*Research Institute, National Cancer Center, Goyang 411-764 South Korea*

[2]*Department of Molecular Cell Biology, Center for Molecular Medicine, Samsung Biomedical Research Institute Sungkyunkwan University School of Medicine, Suwon 440-746, South Korea*

[3]*Korea Institute of Radiological and Medical Sciences, Seoul 139-706, South Korea*

[4]*Division of Molecular and Life Sciences, POSTECH Biotech Center, Pohang University of Science and Technology, Pohang 790-784, South Korea*

[5]*National Institute of Infectious Diseases, Tokyo 162-8640 Japan*

**Corresponding author*

Hepatocellular carcinoma (HCC) is a common primary cancer associated with high incidences of genetic variations including chromosome instability. Moreover, it has been demonstrated that hepatitis C virus (HCV) is one of the major causes of HCC. However, no previous work has assessed whether HCV proteins are associated with the induction of chromosome instability. Here, we found that liver cell lines constitutively expressing full-length or truncated versions of the HCV genome show a high incidence of chromosome instability. In particular, the overexpression of HCV NS5A protein in cultured liver cells was found to promote chromosome instability and aneuploidy. Further experiments showed that NS5A-induced chromosome instability is associated with aberrant mitotic regulations, such as, an unscheduled delay in mitotic exit and other mitotic impairments (e.g. multi-polar spindles). Thus, our results indicate that HCV NS5A protein may be directly involved in the induction of chromosome instability *via* mitotic cell cycle dysregulation, and provide novel insights into the molecular mechanisms of HCV-associated hepatocarcinogenesis.

Keywords: hepatitis C virus; NS5A; mitotic cell cycle; chromosome instability; hepatocellular carcinoma

Introduction

Hepatocellular carcinoma (HCC) is a common primary cancer that is often associated with hepatitis B (HBV) and hepatitis C (HCV) viral infections. In particular, more than 60% of HCV infections lead to chronic hepatitis, which can sequentially progress to chronic active hepatitis, liver cirrhosis, and HCC.[1–3] HCV is an envelope RNA virus and contains a single-stranded positive-sense RNA genome that encodes a precursor polypeptide of approximately 3000 amino acid residues. Host and viral proteases cleave this precursor polypeptide into at least ten individual proteins; namely, core, E1, E2, p7, NS2, NS3, NS4A, NS4B, NS5A and NS5B proteins.[4,5] Moreover, recent studies indicate that HCV viral proteins can play direct roles in oncogenesis.[6–9] For example, transgenic mice harboring HCV core protein, structural proteins, or the full-length genome exhibit marked

Present address: S.- J. Kim, Division of Biology and Biomedical Sciences, Washington University, St Louis, MO 63110-1093, USA.

Abbreviations used: HCV, hepatitis C virus; NS, non-structural; HCC, hepatocellular carcinoma; APC/C, anaphase promoting complex/cyclosome; LOH, loss of heterozygosity; NEBD, nuclear envelope breakdown.

E-mail address of the corresponding author: cwlee@med.skku.ac.kr

liver steatosis and spontaneous HCC development after long periods of latency.[7–9] Interestingly, the development of HCC appears to depend on the host's genetic background, HCV genotype, and the expression levels of introduced HCV genes.[6,10–13] In general, it is believed that HCV proteins significantly cause and/or enhance the risk of liver cancer.

Previous studies suggest that in HCC, neoplastic cells originate from rapidly dividing hepatocytes or liver stem cells that have accumulated genetic alterations and thus demonstrate genomic instability.[14] Moreover, the majority of HCC cells display a high incidence of chromosome instability, including structural chromosomal alterations, and allelic losses and gains. In addition, chromosome instability is evident in cirrhotic liver tissues, and has been found to increase during the hepatocarcinogenesis process.[15,16] Although chromosome aneuploidization is found in many human cancers, it is unclear whether aneuploidy is a consequence of cell transformation, or whether it contributes to tumor progression by increasing tumor suppressor losses and protooncogene gains. Growing evidence indicates that aneuploidy occurs as a result of chromosome missegregation in response to a number of abnormalities, such as, double-strand DNA breaks and the loss of cell cycle checkpoint controls.[17,18] Faithful chromosome segregation is controlled by the mitotic machinery, which includes the kinetochore complex, spindle, centrosome and cohesion complex, and the inactivation or dysregulation of these components causes mitotic defects that can lead to chromosome missegregation and aneuploidy. Although studies have not yet established a direct molecular link between defects in the mitotic checkpoint and aneuploidy in cancer, a growing list of molecular components and processes known to cause chromosome missegregation *in vitro* and *in vivo* may be considered prime candidates.[19–22]

Normally, mitotic checkpoint controls trigger cell cycle arrest and/or the elimination of cells harboring cell cycle defects. However, some cells with constitutive checkpoint defects, such as those caused by DNA tumor virus infections, are able to escape apoptosis and adapt cell cycle progression, thus allowing the continuation of chromosome instability.[23,24] Interestingly, HTLV-1 TAX oncoprotein has been shown to target MAD1 mitotic checkpoint protein, and thus lead to impaired checkpoint function, multi-nucleation, and aneuploidy.[23] Other DNA tumor virus proteins, including E1A and E1B from adenovirus, E6 and E7 from papillomavirus, and large and small T antigens from simian virus 40 (SV40) have been shown to interact with major cellular regulators and induce mitotic abnormalities.[24] Furthermore, HBx protein, which is frequently integrated into the cellular genome, and which is expressed during the HCC development, has been reported to induce centrosome amplification, multi-polar spindles, and aneuploidy.[25] These previous results collectively suggest that mitotic checkpoint impairments may represent a common pathway for viral oncogenesis, and that viral proteins may affect chromosome segregation, leading to mitotic abnormalities and increased aneuploidy.

Previously, Smith *et al.*[14] performed microarray analyses on HCV-associated HCC specimens, and found an association between chromosomal segregation abnormalities and the improper expressions of potential HCC marker genes, such as, Aurora A, CDC2, mitotic cyclins, cyclin-dependent kinases, p53-related genes, and CENP-F. Furthermore, Kawai *et al.*[16] showed that HCC tissues associated with HCV infection show significant losses of heterozygosity (LOH), although the rate of LOH was higher in HBV-associated tissues. Consistent with this finding, LOH was detected more frequently in malignant tumors than in normal liver tissues[26,27] and was almost always accompanied by chromosome instability. These observations raise the possibility that HCV infection may be associated with chromosome instability, which is a known cause of neoplastic degeneration and hepatocarcinogenesis. However, due to the limitations of tissue culture and animal model systems, no previous work has directly examined whether HCV proteins are associated with the induction of chromosome instability.

Here, we examined whether one or more HCV proteins are directly involved in the acquisition of chromosome instability. Our analysis of HCV-associated HCC tumor tissues showed marked chromosomal aberrations, and liver cell lines constitutively expressing full-length or truncated versions of the HCV genome exhibited a high incidence of chromosome instability. In particular, the overexpression of HCV NS5A protein appeared to result in an unscheduled delay in mitotic exit and in mitotic abnormalities (e.g. multi-polar spindles). Moreover, these discrepancies were associated with chromosome instability and aneuploidy in NS5A-expressing cells. These results indicate that there is a direct link between HCV proteins and chromosome aneuploidy in hepatocytes.

Results

HCV non-structural proteins appear to act in an integrated manner during the induction of chromosome instability

Previously, we established stable human hepatoblastoma-derived HepG2 cell lines expressing the entire HCV ORF (Hep394), or ORF fragments including core to NS3 protein (Hep352) or NS2 (C-terminal 52 amino acid residues) to NS5B protein (Hep3294), and used immunochemical analyses to confirm the proper expressions and processing of these proteins in these cell lines.[28] Due to the lack of a cell culture system that supports the efficient propagation of HCV, these cell lines were developed with the intention of providing a suitable

in vitro model of HCV infection. To examine whether HCV proteins are involved in the induction of chromosome instability, we treated parental HepG2 cells or established Hep394, Hep352 or Hep3294 cell lines with colcemid. Giemsa staining was used to visualize chromosomes, which were counted to determine cellular chromosome number distributions (a marker of chromosome instability; Figure 1(a) and (b)). It was found that the Hep394 cell line (expressing the entire HCV ORF) showed a significant increase in cellular chromosome number distribution *versus* parental HepG2 cells. Moreover, Hep3294 cells (expressing NS2 to NS5B proteins) also showed a dramatic increase in cellular chromosome number distribution, whereas Hep352 cells (expressing core to NS3 protein) showed chromosome number distributions similar to those of control HepG2 cells. This observation

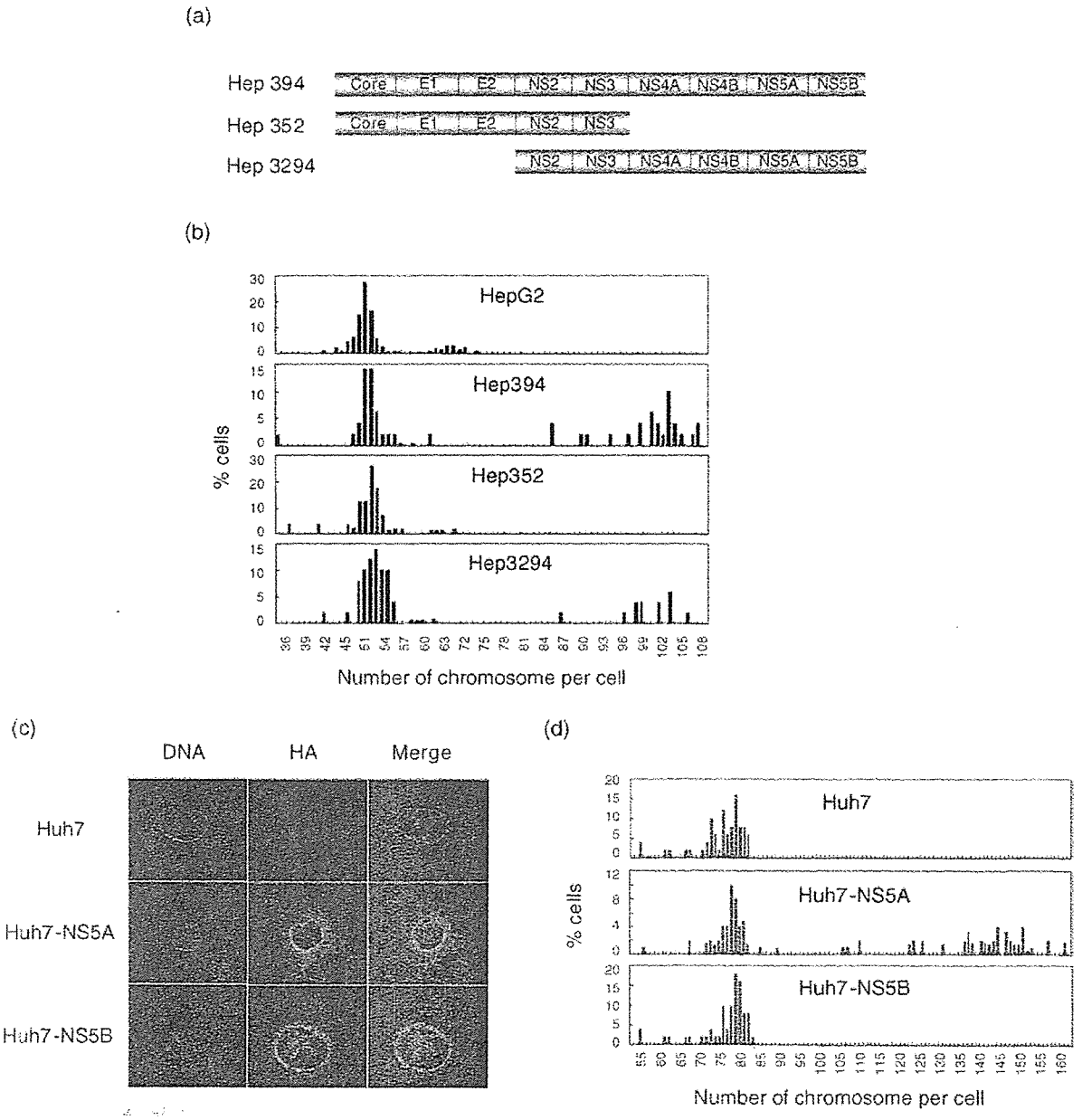

Figure 1. HCV non-structural proteins may be involved in the induction of chromosomal instability. (a) Schematic diagram showing the utilized independent HepG2-based cell lines constitutively expressing the full-length HCV ORF (Hep394), a truncated HCV including the core to NS3 sequences (Hep352), and a truncated HCV including the NS2 to NS5B sequences (Hep3294). The expression and processing of HCV proteins in these cell lines was previously confirmed by biochemical analyses.[28] (b) For metaphase chromosome analysis, parental HepG2 and established clones were cultured and treated with colcemid (0.04 mg/ml), and chromosomes were visualized by Giemsa staining. Chromosome number distributions were counted and analyzed in 200 cells per clone. (c) Expressions of HA-tagged NS5A or NS5B in selected Huh7 cell clones were assayed by immunofluorescence using an anti-HA antibody (red), and DNA was visualized by staining with Hoechst dye (blue). (d) Huh7 clones expressing HA-tagged NS5A (Huh7-NS5A) or NS5B (Huh7-NS5B) and control Huh7 cells were prepared (as described for (b)) for metaphase chromosome spreading analysis. Mitotic cells were randomly selected ($n=200$ per clone) and chromosomes were counted.

provides first evidence that HCV proteins are directly involved in the induction of chromosome instability.

To identify the protein responsible for this effect, we compared the effects of expression plasmids encoding NS4A/4B or NS5A and NS5B on hepatocyte growth. Consistent with the previous findings,[29] flow cytometry revealed that cells co-transfected with NS5A and NS5B expression plasmids exhibited a shortened S phase and a significantly increased proportion of cells arrested in the G2 and M phases, as compared to cells transfected with NS4A/4B alone or with empty vector (data not shown), indicating that NS5A and/or NS5B may affect the cell cycle by regulating chromosome replication or chromosome segregation. To address whether HCV proteins, especially NS5A and NS5B, play roles in chromosomal instability and aneuploidy, we generated stable cell lines expressing HCV NS5A and NS5B in HBV genome-negative hepatocellular carcinoma-derived Huh7 cells (Figure 1(c) and (d)). Individual G418-resistant stable Huh7 cell clones were screened for NS5A and NS5B expression by immunofluorescence (Figure 1(c)) and immunoblotting (data not shown) using an anti-HA antibody. The data described below were obtained using single clones showing moderate levels of NS5A or NS5B expression, and all results were confirmed by examining two additional independent clones per cell line. NS5A-expressing and control Huh7 cells were cultured, treated with colcemid and subjected to Giemsa staining. As shown in Figure 1(d), Huh7-NS5A cells showed markedly increased chromosomal number distributions (143–155 chromosomes in ~60% of cells) as compared with control Huh7 cells grown under the same conditions (72–82 chromosomes in ~80% of cells). In contrast, Huh7-NS5B cells showed virtually the same chromosome number distribution profile as control Huh7 cells. To rule out the possibility that the induction of chromosome instability by NS5A protein may have been dependent on the cell line used, we performed parallel experiments in control Chang-HA (empty vector-transfected) and Chang-NS5A cells. As expected, chromosome spreading analysis revealed that Chang-NS5A cells showed a significantly higher incidence of chromosome instability than the control Chang-HA cells (data not shown). Collectively, these results demonstrate that HCV NS5A protein expression induces chromosomal instability.

HCV NS5A protein expression affects the normal timing of mitotic progression by delaying mitotic exit

Aberrant chromosome distributions were observed in cells expressing HCV NS5A, and thus we compared cell cycle progressions through S, G2, and mitosis (M) in the established Chang clones, i.e. vector-transfected control Chang-HA cells, Chang-NS5A cells, and Chang-NS5B cells (Figure 2(a)). Cells were synchronized at the G1/S boundary using a double thymidine block, and following release from G1/S arrest cells were harvested and analyzed for DNA content by flow cytometry (Figure 2(b)). Interestingly, at 10 h and 12 h after release, cells expressing NS5A showed a significant delay in mitotic exit, as evidenced by an accumulation of cells at G2/M and a decrease in the G1 population. In contrast to Chang-NS5A, Chang-NS5B cells and control Chang-HA cells progressed similarly. To determine whether NS5A expression is associated with the accumulation of cells in G2 or M, we treated cells with nocodazole and monitored the populations of MPM2-positive cells (an indicator of the mitotic phase of the cell cycle) (Figure 2(c)). In control Chang cells, mitotic indexes increased rapidly from 12 h to 24 h after nocodazole treatment and then decreased sharply at 36 h post-treatment. In contrast, cells expressing NS5A protein maintained a constant mitotic index for up to 36 h after nocodazole treatment, indicating that NS5A protein expression interferes with the normal timing of mitotic cell cycle progression by delaying mitotic exit. Next, we observed the effect of NS5A protein expression on the timing and morphology of NS5A-expressing mitotic cells using time-lapse photomicroscopy at 2 min intervals. As each cell entered mitosis, nuclear envelope breakdown (NEBD) was set as time zero, and the relative times for individual cell types to complete chromosome separation were then determined (Figure 2(d)). In control Chang-HA cells, the time to completion of chromosome separation was 67.6($\pm$12.6) min (Figure 2(e)). Interestingly, NS5A-expressing cells showed a significant retardation of mitotic cell cycle progress, with an 86.2($\pm$31.3) min interval between NEBD and complete chromosome separation (Figure 2(e)). In addition, a significant proportion of NS5A-expressing cells failed to complete chromosome separation over the duration of imaging (4 h); 57% of Chang-NS5A cells remained in metaphase at the end of observation period as compared with only 10% of Chang-HA cells (Figure 2(f)). These results collectively indicate that NS5A-expressing cells remain arrested in mitosis for an abnormally long time, thus delaying chromosome separation.

Delayed mitotic exit induced by NS5A expression may be associated with mitotic abnormalities

Normal cells display two centrosomes and two spindle poles during mitosis, ensuring bipolar microtubule attachment to sister chromatids, and abnormal centrosomes or mitotic spindles lead to unequal chromosome segregation and subsequent aneuploidy. Thus, since NS5A protein overexpression delays mitotic exit, it is possible that NS5A protein contributes to mitotic machinery defects associated with chromosome missegregation. Therefore, we examined whether aberrant mitotic arrest by NS5A overexpression is related to mitotic

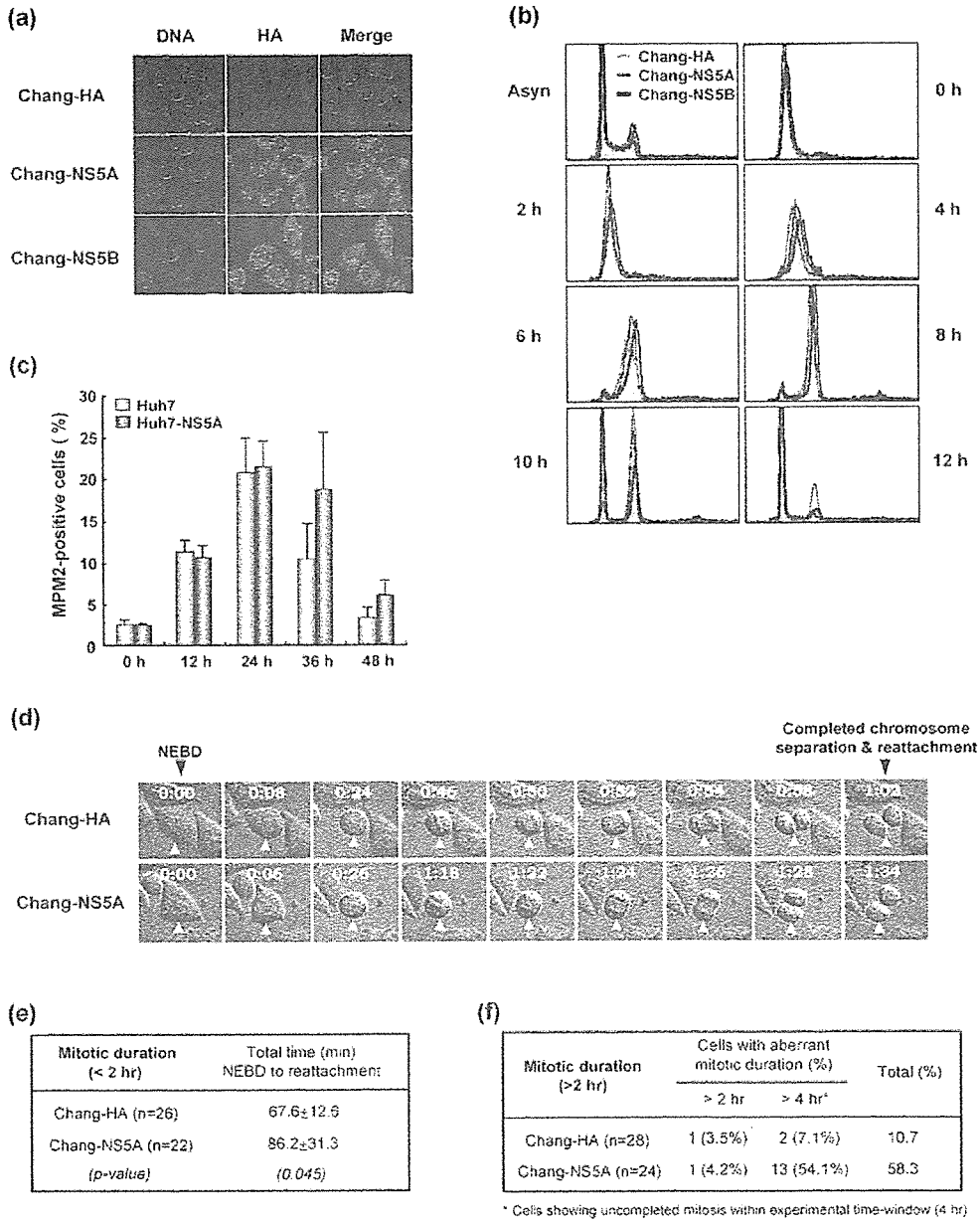

(e)

Mitotic duration (< 2 hr)	Total time (min) NEBD to reattachment
Chang-HA (n=26)	67.6±12.6
Chang-NS5A (n=22)	86.2±31.3
(p-value)	*(0.045)*

(f)

Mitotic duration (>2 hr)	Cells with aberrant mitotic duration (%)		Total (%)
	> 2 hr	> 4 hr*	
Chang-HA (n=28)	1 (3.5%)	2 (7.1%)	10.7
Chang-NS5A (n=24)	1 (4.2%)	13 (54.1%)	58.3

* Cells showing uncompleted mitosis within experimental time-window (4 hr)

Figure 2. Exogenous expression of HCV NS5A protein results in delayed mitotic exit. (a) Expression of HA-tagged NS5A (Chang-NS5A) or NS5B (Chang-NS5B) in selected Chang cell clones was assayed by immunofluorescence using an anti-HA antibody (green) and Hoechst dye (blue). (b) Chang liver cells expressing NS5A (Chang-NS5A, red) or NS5B (Chang-NS5B, green) and empty vector-transfected control cells (Chang-HA, gray) were synchronized at the G1/S boundary by a double thymidine block (see Materials and Methods). After release from G1/S arrest, cells were harvested and subjected to flow cytometry at the indicated time points. Asyn indicates asynchronized cells. (c) Control Chang-HA and Chang-NS5A cells were treated with nocodazole, harvested, stained with PI and an FITC-conjugated anti-MPM2 antibody, and examined by flow cytometry. Distributions of MPM2-positive cells after nocodazole treatment were graphed based on comparisons between Chang-HA and Chang-NS5A cells. The values shown are the means of three independent experiments, and bars indicate standard deviations. (d) Chang-HA and Chang-NS5A cells were cultured and imaged by time-lapse photomicroscopy during mitotic progression; nuclear envelope breakdown (NEBD) was designated time zero. Times from NEBD to complete chromosome separation were measured (an example is indicated by the arrowhead). Representative time-lapse images are shown. (e) Mitotic progression data from randomly selected Chang-HA and Chang-NS5A cells obtained from the image in (d). The percentages of cells showing aberrant mitotic durations of less than 2 h were compared. *P*-values were obtained using the Student's *t* test. (f) Percentages denote the population of cells showing incomplete mitosis at 4 h.

abnormalities, such as mitotic spindle defects, abnormal centrosome formation, or cytokinesis failure. Immunofluorescence analyses using α-tubulin and γ-tubulin were used to visualize mitotic spindles and centrosomes, respectively, in NS5A-expressing and control cells (Figure 3(a)). Interestingly, Huh7-NS5A cells exhibited microtubule disarray and increased numbers of cells

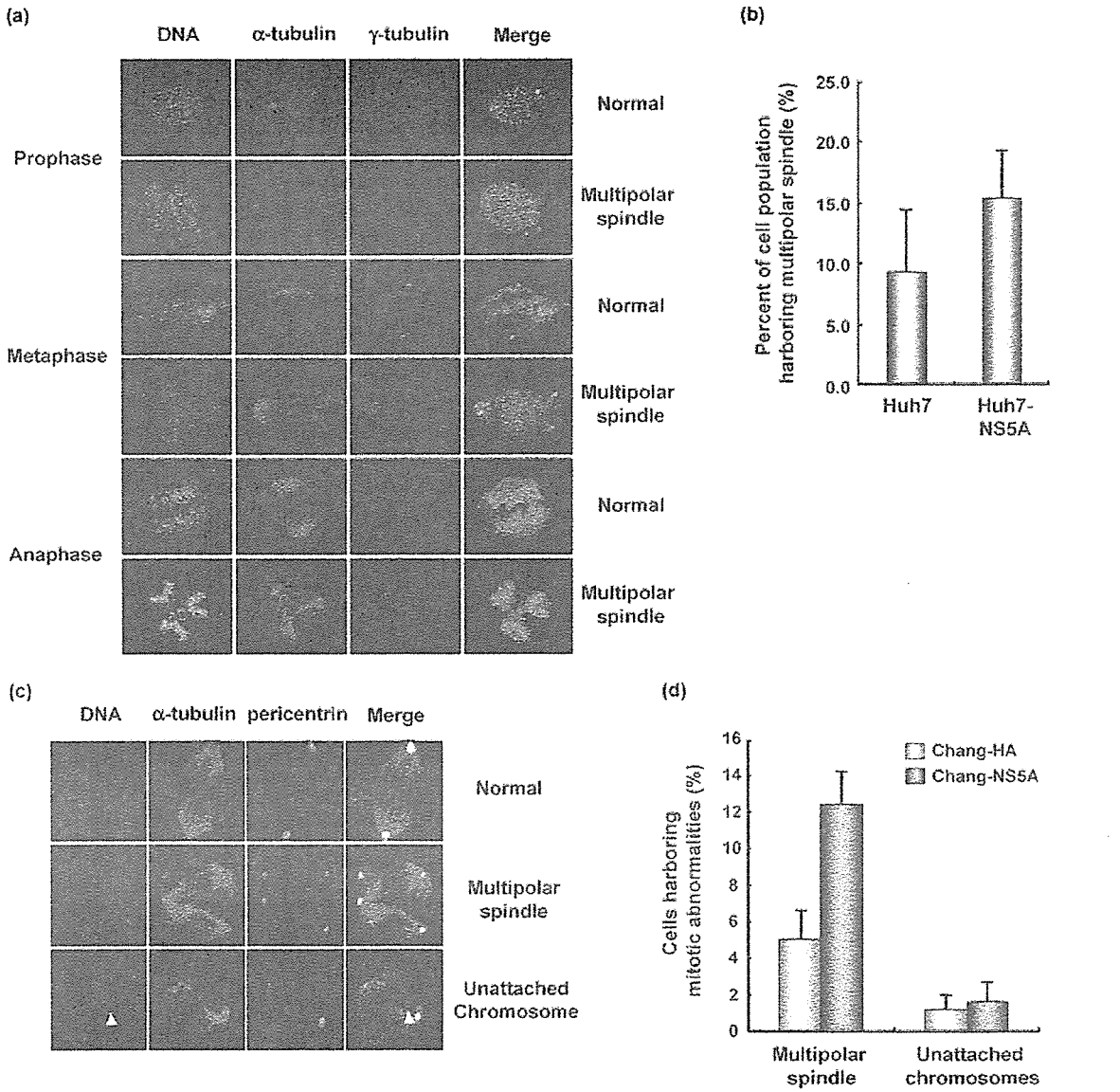

Figure 3. Cells expressing NS5A exhibited more mitotic spindle assembly defects. (a) To analyze mitotic spindles, control Huh7 and Huh7-NS5A cells were co-immunostained with anti-α-tubulin (green) and anti-γ-tubulin (red) antibodies. DNA was visualized with Hoechst dye (blue). Representative confocal microscopic images are shown. More than two centrosomes and spindles per cell were considered to indicate multi-polar (abnormal) spindles. (b) Graphical comparison of multi-polar spindle numbers in Huh7 and Huh7-NS5A cells. The values shown are the means of three independent experiments, in which more than 300 mitotic phase cells were counted, and bars indicate standard deviations. (c) Control Chang-HA and Chang-NS5A cells were co-immunostained with anti-α-tubulin (green) and anti-pericentrin (red) antibodies and DNA was visualized with Hoechst dye (blue). Populations of cells harboring mitotic abnormalities were determined by the presence of multi-polar spindles and/or unattached chromosomes. Representative confocal microscopic images are shown. The arrowhead designates unattached chromosomes. (d) Profiles of mitotic abnormalities in Chang-HA and Chang-NS5A cells. The frequencies of multi-polar spindles and unattached chromosomes were estimated from three independent experiments during which more than 331 mitotic phase cells were counted.

with more than two centrosomes and mitotic spindle poles (~15.5% of cells) as compared to vector-transfected control cells (~8.5%) (Figure 3(b)), suggesting that cells expressing NS5A protein show mitotic machinery abnormalities. Similarly, we immunoassayed control Chang-HA and Chang-NS5A cells using antibodies against α-tubulin and pericentrin (Figure 3(c)), and found that about 14% of NS5A-expressing cells displayed multi-polar spindles as compared with about 4% of control Chang cells (Figure 3(d)). The overexpression of NS5A also slightly increased the population of cells with unattached chromosomes (Figure 3(d)). In addition, recent reports show that cytokinesis failure and subsequent binucleation result in tetraploidization, which frequently is able to proceed to aneuploidy.[30,31] Therefore, we investigated whether the overexpression of NS5A contributes to cytokinesis failure and binucleation. However, cells expressing NS5A showed no

significant difference in the population of binucleated cells compared with control cells (see Supplementary Data, Figure S1). Together, these observations indicate that the overexpression of HCV NS5A is correlated with an increase in the number of cells with mitotic spindles and centrosomes rather than unsuccessful cytokinesis and binucleation.

Next, we compared the expression profiles of mitotic marker proteins, such as phospho-H3, Aurora A, Cyclin A, Cyclin B1, and BubR1, in control Huh7 and Huh7-NS5A cells. Huh7 and Huh7-NS5A cells were cultured in the presence of nocodazole, and cell extracts were prepared at the indicated time-points and resolved by gel electrophoresis at equal loading quantities. Levels of the indicated proteins were assessed by immunoblotting using anti-HA, anti-phospho-H3, anti-Aurora A, anti-Cyclin A, anti-Cyclin B1, anti-BubR1, anti-Cdh1 and anti-Actin antibodies (Figure 4). In control Huh7 cells, phosphorylation of histone H3 was induced at 12 h after nocodazole treatment, peaked at 30 h, and then rapidly decreased (Figure 4(a)), whereas in NS5A-expressing cells, histone H3 phosphorylation was induced at 6 h and maintained for up to 42 h after nocodazole treatment (Figure 4(a)). Because histone H3 phosphorylation occurs during mitosis and is required for proper chromosome condensation and segregation, this result confirms that NS5A protein expression increases the population of cells aberrantly arrested in mitosis. In addition, we examined the expressions of Cyclin A, Cyclin B1, and Aurora A, which play important roles in initiating and maintaining mitotic cell cycle control *via* their specifically timed expressions

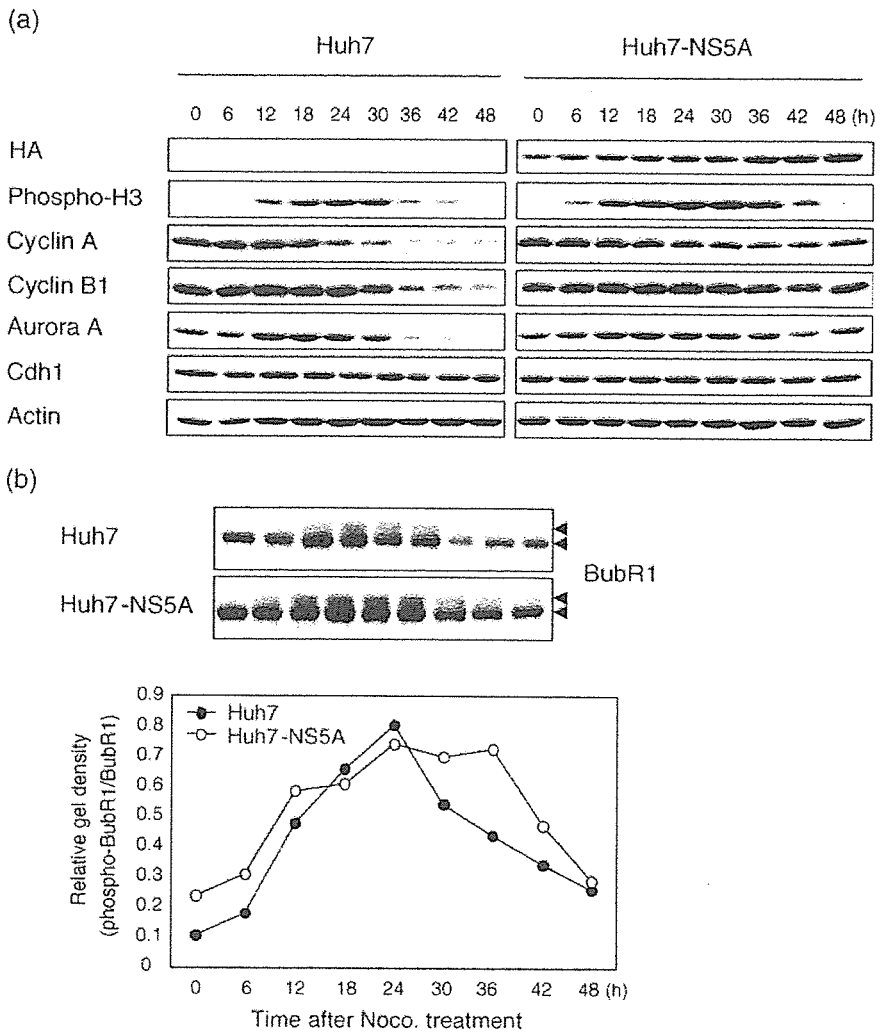

Figure 4. Cells expressing NS5A remained in mitotic arrest for an extended duration. (a) and (b) Huh7 and Huh7-NS5A cells were cultured in the presence of nocodazole (0.1 μg/ml). Cell extracts were prepared at the indicated time-points and were resolved by gel electrophoresis at equal loadings. Levels of the indicated proteins were assessed by immunoblotting using anti-HA, anti-phospho-H3, anti-Aurora A, anti-Cyclin A, anti-Cyclin B1, anti-BubR1, anti-Cdh1, or anti-Actin antibodies. Profiles of BubR1 phosphorylation status in Huh7 and Huh7-NS5A cells are presented as relative gel densities (b). Gel densities of hyperphosphorylated BubR1 (upper arrowhead) and hypophosphorylated BubR1 (lower arrowhead) were quantified by densitometry, and values were obtained by dividing the gel densities of hyperphosphorylated BubR1 by those of hypophosphorylated BubR1.

and degradations (Figure 4(a)). In particular, Cyclin A is destabilized when cells enter mitosis, and is almost completely degraded before the metaphase to anaphase transition.[32–34] Moreover, Cyclin B1 degradation is required for the transition from metaphase into anaphase.[32–34] We found that Cyclin A levels began to decrease 30 h after nocodazole treatment in Huh7 cells, but remained stable for up to 48 h in Huh7-NS5A cells, whereas Cyclin B1 levels decreased at 36 h after nocodazole treatment in Huh7 cells, but accumulated in Huh7-NS5A cells over the entire experimental time course (up to 48 h). On the other hand, Aurora A levels decreased consistently from 36 h after nocodazole treatment in Huh7 cells, but were maintained in Huh7-NS5A cells. Finally, we compared the phosphorylation status of BubR1 protein, because the hyperphosphorylation of BubR1 is known to be a prerequisite of exit from mitotic arrest.[35] In control cells, the hyperphosphorylated form of BubR1 increased from 12 h after nocodazole treatment, peaked at 24 h, and then rapidly decreased (Figure 4(b)). However, in cells expressing NS5A, hyperphosphorylation of BubR1 was detectable from 6 h after treatment and was maintained for up to 42 h (Figure 4(b)). These results collectively indicate that cells expressing NS5A cause aberrant elevations of these mitotic marker proteins and thus perturb the normal timing of the mitotic cell cycle.

Overexpression of HCV NS5A protein induces chromosome aneuploidy

Following prolonged mitotic arrest in response to spindle damage, even cells possessing a competent mitotic checkpoint eventually exit mitosis and undergo apoptosis. However, cells with a persistent mitotic abnormality, such as mutational inactivation of a mitotic checkpoint gene, tend to escape apoptosis and continue cell cycle progression.[21,36–38] Therefore, we questioned whether the aberrant mitotic arrest and mitotic abnormalities induced by NS5A expression could contribute to chromosome missegregation and subsequent aneuploidy. Thus, we treated asynchronized control Huh7 and Huh7-NS5A cells with a microtubule inhibitor (nocodazole) and harvested the cells at various time-points (Figure 5(a)). Interestingly, whereas control Huh7 cells showed marked increases in apoptotic cell populations, Huh7-NS5A cells showed significant increases in aneuploid cells, and these increases were seemingly correlated with duration of exposure to the microtubule inhibitor. In contrast, Huh7-NS5B cells showed reduced apoptosis and increased numbers of cells arrested in the G2/M phases, but no significant accumulation of aneuploid cells (data not shown). To confirm these results, we performed parallel experiments in control Chang-HA and Chang-NS5A cells. As expected, flow cytometric analysis revealed that

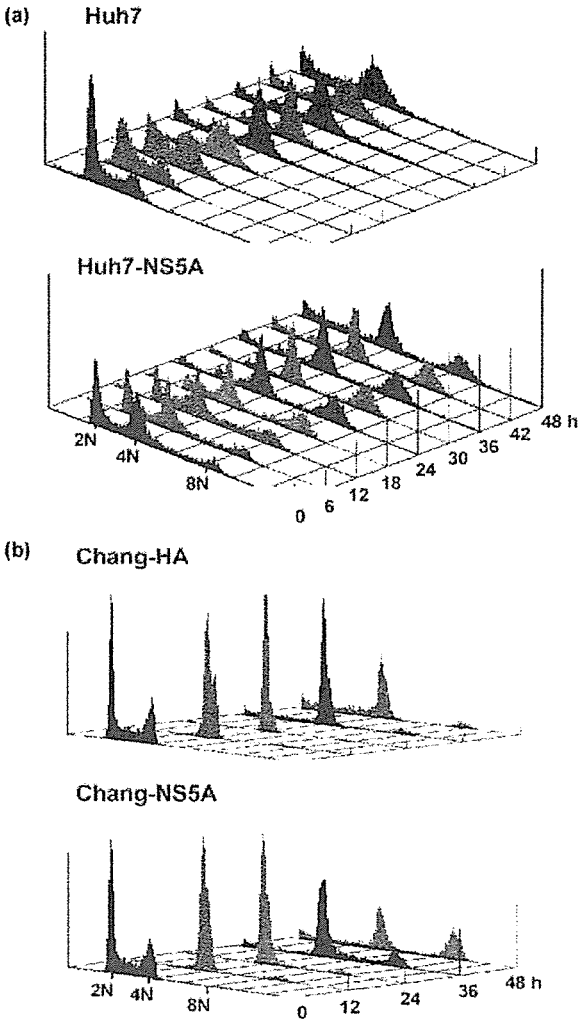

Figure 5. Exogenous expression of HCV NS5A protein induces chromosome aneuploidy. (a) Asynchronized control Huh7 and Huh7-NS5A and (b) Chang-HA and Chang-NS5A cells were treated with nocodazole (0.1 μg/ml). At the indicated time-points, cells were harvested, stained with propidium iodide, and analyzed for DNA content by flow cytometry.

Chang-NS5A cells showed significant accumulations of aneuploid cells compared with control Chang-HA cells (Figure 5(b)). Collectively, our results demonstrate that the expression of HCV NS5A protein induces aneuploidy, and that this appears to be associated with mitotic abnormalities, such as delayed mitotic exit and multi-polar spindle formation.

HCV infection may be directly associated with chromosomal instability

It has been shown that array-based comparative genomic hybridization (CGH) can detect the chromosome aberrations characteristic of human tumors.[39] Here, tumor tissues and adjacent non-tumor tissues were obtained from five HCV-infected patients, all of whom were positive for

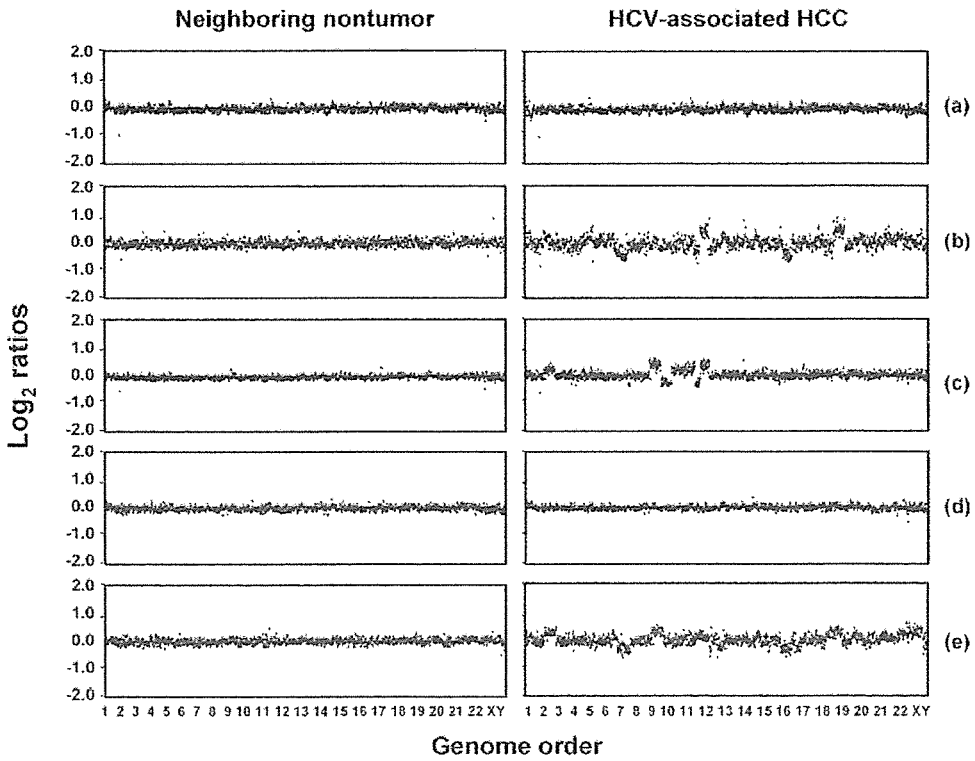

Figure 6. Detection of chromosome aberrations in HCV-associated HCC tumors using CGH arrays. Genomic DNA was isolated from frozen HCV-associated (left panels) and adjacent non-tumor (right panels) tissues from five patients, and subjected to whole genome CGH array analysis with fluorescent *in situ* hybridization (see Materials and Methods). The measured $\log_2$ ratios of the Cy3/Cy5 fluorescence intensities of spots ranged from +0.2 to −0.2. Threshold levels for $\log_2$ ratio gains and losses were set at +0.2 and −0.2, respectively. The *y*-axis indicates the $\log_2$ ratio of quadruplicate measurements per chromosome, and shows chromosome gains or losses. Chromosomes are shown on the *x*-axis, in order from 1p to Xq/Yq. A blinded CGH array study revealed widespread chromosomal aberrations in three of five cases ((b), (c) and (e)).

anti-HCV antibody (HCV-Ab) and HCV RNA, but negative for hepatitis B surface antigen (HBs-Ag). The CGH profiles of these samples are shown in Figure 6. Interestingly, three of the five HCV-associated HCC tumors ((b), (c) and (e)) showed marked chromosome instability, as indicated by widespread chromosome copy number abnormalities. In contrast, no significant indication of widespread genomic alterations was evident in the five adjacent non-tumor tissue samples. Consistent with speculations in previous studies,[16,26,27] these observations provide evidence that HCV infection may be directly associated with chromosomal instability.

Discussion

Here, we provide novel evidence that indicates that cells expressing HCV polyproteins induce chromosomal instability. Furthermore, our findings demonstrate that cells expressing NS5A protein show delayed mitotic exit and mitotic apparatus abnormalities (i.e. multi-polar spindles), which enable cells with unbalanced sets of chromatids segregated at multiple spindle poles to progress to anaphase and telophase. Importantly, we observed similar phenotypes in human primary cells, lung L132 cells, and amniocytes (A139 cell line), by monitoring the ectopic expression of NS5A using a recombinant adenovirus (see Supplementary Data, Figure S2). Thus, repeated failure of balanced chromatids segregation due to persistent HCV protein expression appears to cause widespread chromosome instability and aneuploidy in hepatocytes. During prolonged mitotic arrest, mitotic checkpoint components have been shown to inhibit APC/C, and to prevent it from targeting Cyclin B1 and Securin for degradation.[40] In the present work, we found that NS5A-expressing cells showed increased fractions of mitotic cells and reduced populations of G1 cells, and reduced degradations of APC/C substrates, Cyclin B1 (Figure 4) and Securin (data not shown). These observations indicate that NS5A may be involved in the unscheduled activation of APC/C, and thus, the development of aneuploidy. However, additional study is required to identify the cellular factors targeted by NS5A in this context.

It is widely believed that cells with mitotic abnormalities produce a "wait signal" to delay the onset of anaphase, and that a "fail-safe" mechanism exists to trigger apoptosis in cells that breach the mitotic checkpoint, thus avoiding aneuploidy. However, our results indicate that cells expressing

HCV non-structural proteins somehow adapt to aneuploidy and return to the cell cycle following a sustained mitotic delay. Recent studies have suggested that NS5A exerts an anti-apoptotic effect, and thus confers a viral multiplicative potential in infected cells. In addition, it has been reported that NS5A activates NF-*k*B by inducing oxidative stress in cells.[41] Moreover, liver tissues from chronic hepatitis C patients displayed elevated levels of NF-*k*B[42] and NF-*k*B was shown to induce the expressions of anti-apoptotic factors, such as IAP and Bcl-2.[43] Therefore, it is likely that the persistent expression of NS5A triggers or maintains the expressions of genes that provide protection against apoptotic stimuli, perhaps even during the acute phase of liver disease associated with HCV infection. Consistent with this notion, we observed that cells expressing HCV NS5A and NS5B showed caspase-3 activation inhibition following nocodazole treatment, whereas control cells showed activation of the apoptotic pathway upstream of caspase-9, which sequentially activates caspase-3 (data not shown). Thus, it appears that HCV NS5A interferes with "gatekeeper" cellular functions by blocking apoptotic pathways, thereby enabling cells with mitotic abnormalities and aneuploidy to continue cycling.

HCC tumors are associated with high incidences of genetic alterations, which increase during the carcinogenic process. Moreover, it is known that chronic liver injury caused by HCV infection eventually leads to necrosis, inflammation, and liver regeneration, and that it is frequently associated with an accumulation of genetic alterations, such as, loss of p53 function.[44–46] Cells lacking functional p53 undergo normal mitotic arrest in response to spindle damage, but then subsequently avoid the checkpoint, enter S phase, and endoreduplicate DNA, resulting in aneuploidy.[47] Thus, p53 protein appears to be required to protect normal cells from adaptation to chromosomal instability. In addition, a variety of other genetic and epigenetic aberrations at various stages may collaborate to allow adaptation and aneuploidy. For example, the overexpression of Aurora A (a centrosome-associated serine/threonine kinase) has been implicated in chromosome segregation abnormalities and aneuploidy in many cancer cell types.[48] Smith *et al.*[14] found that Aurora A was upregulated in about 85% of HCV-associated hepatocellular carcinoma tumor samples, and further, the overexpression of Aurora A has been reported to override the mitotic checkpoint and to lead to the premature mitotic exit of cells with inappropriately aligned chromosomes.[49] In the present work, we found that NS5A-expressing cells offered resistance to the normal mitotic cell cycle-dependent destabilization of Aurora A (see Supplementary Data). This suggests that the deregulation of cellular factors, such as Aurora A, acts in concert with HCV non-structural proteins to induce mitotic abnormalities and aneuploidy. However, a previous study provided important evidence that the non-structural proteins of HCV may contribute to hepatic carcinogenesis, whereas structural proteins are a risk factor for the development of steatosis but not liver cancer,[7] which seems to suggest that HCV non-structural proteins are associated with chromosomal instability. In the present study, the frequency and extent of chromosome instability in NS5A-expressing cells was abnormally high even in the absence of a mitotic cell cycle-deregulating stimulus (i.e. nocodazole) (Figure 4), which implies that HCV NS5A protein directly interferes with the normal timing of the mitotic process *in vitro*. However, it should be noted that levels of HCV proteins are very low *in vivo*, i.e. they are not easily detected by routine immunohistochemical assays of HCV-infected liver samples. Thus, NS5A alone may not be sufficient to trigger mitotic abnormalities *in vivo* and other factors may be required to facilitate NS5A-induced aneuploidy. In agreement with a previous report,[29] we also found that NS5B triggers cell cycle arrest in G2, although this aberrant cell cycle arrest was not linked to a mitotic abnormality or chromosomal instability. Thus, our findings suggest that NS5B may help extend the aberrant cell cycle arrest required for adaptation. Moreover, NS5A has been shown to interact functionally with NS5B,[50,51] thus indicating that this non-structural protein may cooperate in HCV-induced mitotic impairments. However, additional work is required to establish a functional link between NS5A and NS5B with respect to hepatocyte mitotic behavior.

The present study demonstrates for the first time that HCV proteins interrupt the normal timing of the mitotic cell cycle and induce the chromosome instability that is frequently observed in malignant tumors. These findings provide important new insights into HCV-associated hepatocarcinogenesis, and may provide a basis for future therapeutic strategies.

Materials and Methods

Generation of cell lines

Human hepatoma-derived cell lines constitutively expressing full-length (Hep394) or fragments of the HCV open reading frame (Hep352 and Hep3294) were generated as described.[28] To generate liver cell lines expressing HA-tagged NS5A and NS5B, HCV genotype 1b cDNAs encoding NS5A and NS5B were inserted into the pCMV-HA vector,[52] and Huh-7 and Chang liver cells were transfected with the constructs or with empty vector (control). Colonies resistant to G418 (GIBCO BRL) were clonally isolated and screened for expression of NS5A or NS5B, using immunoblot and immunofluorescence assays with an anti-HA antibody (Roche).

Chromosome spreading analysis

For cytogenetic analysis of metaphase chromosomes, established cells were incubated with colcemid (0.04 mg/ml) for 4 h, treated with 0.56% (w/v) KCl for 5 min and fixed with methanol/glacial acetic acid (3:1 (v/v)).

Chromosomes were visualized by Giemsa staining and microscopy.

Cell cycle analysis

For flow cytometric analysis of cell cycle profiles, 10^6 cells were plated in 10 cm dishes and cultured in the presence of 0.1 μg/ml nocodazole (Sigma). At the indicated times, cells were harvested, fixed in 70% (v/v) ethanol, washed in phosphate-buffered saline (PBS), and stained with 40 μg/ml propidium iodide (PI) in the presence of 50 μg/ml RNase A for 30 min at room temperature. Samples of 10,000 cells were then analyzed on a Becton Dickinson FACScan flow cytometer (BD Biosciences) and the data were analyzed with the CellQuest software (BD Biosciences). To generate synchronized populations, established clones were arrested at the G1/S boundary by a double thymidine block[34] and then released. At various time-points after release, cells were harvested and analyzed.

For determination of the mitotic index of each population, cells were harvested, resuspended in Cytofix/Cytoperm™ solution (BD Biosciences Pharmingen), washed with Perm/Wash™ buffer (BD Biosciences Pharmingen), and stained with an anti-MPM2 antibody (Dako) in the presence of PI (10 μg/ml final concentration). Samples of 10,000 cells were then subjected to flow cytometric analysis on a FACScan (as above).

Immunoblot analysis

For immunoblot analysis, cells were cultured as described above and then harvested and lysed at the indicated times. Equal amounts of whole cell proteins were resolved by SDS-PAGE, transferred to a nitrocellulose membrane, blocked, and analyzed with anti-phospho-Histone H3 (Upstate Biotechnology), anti-Aurora A (Abcam), anti-Cyclin A (Santa Cruz Biotechnology), anti-Cyclin B1 (Santa Cruz Biotechnology), anti-BubR1 (BD Biosciences Pharmingen), anti-Cdh1 (Oncogene Research Products), or anti-Actin (Sigma) antibodies.

Live cell imaging

To estimate the duration of mitosis, live cells were imaged in ΔT 0.15 mm dishes (IWAKI) in CO_2-independent medium (GIBCO BRL) supplemented with 10% FBS at 37 °C. Every 2 min for 6 h, 0.5 s exposures were acquired using a 20× NA0.75 objective on an LSM 500 META confocal microscope (Carl Zeiss).

Immunofluorescence

Cells were cultured on 18 mm cover-slips, fixed in 5% (v/v) formaldehyde for 10 min, and permeabilized in PBS containing 0.1% Triton X-100 for 5 min. For examination of the sub-cellular localization of HA-tagged NS5A and NS5B, cells were incubated with anti-HA antibody at room temperature for 2 h followed by a further incubation with anti-mouse IgG conjugated with Alexa Fluor 488 (Molecular Probes) for 1 h. To visualize centrosomes and mitotic spindles, cells were incubated with anti-α-tubulin-FITC (Sigma) and anti-γ-tubulin-Cy3 (Sigma) or pericentrin (Abcam) antibodies, respectively, at room temperature for 1 h. Finally, cells were washed, exposed to Hoechst dye for visualization of DNA, and then viewed under an LSM 500 META confocal microscope.

Liver tissue samples and comparative genomic hybridization (CGH)

Surgically dissected materials were collected from patients at the National Cancer Center (NCC), Korea. Informed consent was obtained and specimens were used in accordance with the guidelines of the NCC Tumor Bank Review Committee. Tumor and adjacent non-tumor tissues were sampled from five patients subsequently found to be positive for the anti-HCV antibody (HCV-Ab; LG Biotech) and HCV RNA (Biosewoom), but negative for the hepatitis B surface antigen (HBs-Ag, Bayer).

Tissues were frozen and genomic DNA was isolated with the PUREGENE DNA isolation kit (Gentra). Probes were directly labeled with Cy3-conjugated dUTP and Cy5-conjugated dUTP for the test and reference DNA samples, respectively, using random prime labeling (Invitrogen). Labeled probes were purified and eluted with spin columns (Qiagen), and then hybridized to an array consisting of 1440 BAC clones (350 cancer-related genes and unique STSs with cytological locations confirmed by FISH; GenomArray™, Macrogen†). The hybridization, washing, scanning and analysis were performed according to the GenomArray™ user's manual. Ten simultaneous hybridizations of HCV-associated tumor specimens *versus* the neighboring non-tumor tissues were performed to define the $\log_2$ ratio.

Acknowledgements

We thank members of the laboratory of Chang-Woo Lee for helpful discussions. This work was supported by research grants from the National Cancer Center, Korea and the Korea Health 21 R&D Project, Ministry of Health & Welfare (03-PJ10-PG13-GD01-0002).

Supplementary Data

Supplementary data associated with this article can be found, in the online version, at doi:10.1016/j.jmb.2006.03.020

References

1. Hoofnagle, J. H. (1997). Hepatitis C: the clinical spectrum of disease. *Hepatology*, **26**, S15–S20.
2. Llovet, J. M., Burrough, A. & Bruix, J. (2004). Hepatocellular carcinoma. *Lancet*, **362**, 1907–1917.
3. Zoulim, F., Chevallier, M., Maynard, M. & Trepo, C. (2003). Clinical consequences of hepatitis C virus infection. *Rev. Med. Virol.* **13**, 57–68.
4. Bartenschlager, R. & Lohmann, V. (2000). Replication of hepatitis C virus. *J. Gen. Virol.* **81**, 1631–1648.
5. Penin, F., Dubuisson, J., Rey, F. A., Moradpour, D. & Pawlotsky, J. M. (2004). Structural biology of hepatitis C virus. *Hepatology*, **39**, 5–19.

† http://bac.macrogen.com

6. Kato, T., Miyamoto, M., Date, T., Yasui, K., Taya, C., Yonekawa, H. *et al.* (2003). Repeated hepatocyte injury promotes hepatic tumorigenesis in hepatitis C virus transgenic mice. *Cancer Sci.* **94**, 679–685.
7. Lerat, H., Honda, M., Beard, M. R., Loesch, K., Sun, J., Yang, Y. *et al.* (2002). Steatosis and liver cancer in transgenic mice expressing the structural and non-structural proteins of hepatitis C virus. *Gastroenterology*, **122**, 352–365.
8. Moriya, K., Fujie, H., Shintani, Y., Yotsuyanagi, H., Tsutsumi, T., Ishibashi, K. *et al.* (1998). The core protein of hepatitis C virus induces hepatocellular carcinoma in transgenic mice. *Nature Med.* **4**, 1065–1067.
9. Moriya, K., Nakagawa, K., Santa, T., Shintani, Y., Fujie, H., Miyoshi, H. *et al.* (2001). Oxidative stress in the absence of inflammation in a mouse model for hepatitis C virus-associated hepatocarcinogenesis. *Cancer Res.* **61**, 4365–4370.
10. Honda, A., Arai, Y., Hirota, N., Sato, T., Ikegaki, J., Koizumi, T. *et al.* (1999). Hepatitis C virus structural proteins induce liver cell injury in transgenic mice. *J. Med. Virol.* **59**, 281–289.
11. Kawamura, T., Furusaka, A., Koziel, M. J., Chung, R. T., Wang, T. C., Schmidt, E. V. & Liang, T. J. (1997). Transgenic expression of hepatitis C virus structural proteins in the mouse. *Hepatology*, **25**, 1014–1021.
12. Matsuda, J., Suzuki, M., Nozaki, C., Shinya, N., Tashiro, K., Mizuno, K. *et al.* (1998). Transgenic mouse expressing a full-length hepatitis C virus cDNA. *Jpn. J. Cancer Res.* **89**, 150–158.
13. Pasquinelli, C., Shoenberger, J. M., Chung, J., Chang, K. M., Guidotti, L. G., Selby, M. *et al.* (1997). Hepatitis C virus core and E2 protein expression in transgenic mice. *Hepatology*, **25**, 719–727.
14. Smith, M. W., Yue, Z. N., Geiss, G. K., Sadovnikova, N. Y., Carter, V. S., Boix, L. *et al.* (2003). Identification of novel tumor markers in hepatitis C virus-associated hepatocellular carcinoma. *Cancer Res.* **63**, 859–864.
15. Attallah, A. M., Tabll, A. A., Salem, S. F., El-Sadany, M., Ibrahim, T. A., Osman, S. & El-Dosoky, I. M. (1999). DNA ploidy of liver biopsies from patients with liver cirrhosis and hepatocellular carcinoma: a flow cytometric analysis. *Cancer Letters*, **142**, 65–69.
16. Kawai, H., Suda, T., Aoyagi, Y., Isokawa, O., Mita, Y., Waguri, N. *et al.* (2000). Quantitative evaluation of genomic instability as a possible predictor for development of hepatocellular carcinoma: comparison of loss of heterozygosity and replication error. *Hepatology*, **31**, 1246–1250.
17. Lengauer, C., Kinzler, K. W. & Vogelstein, B. (1998). Genetic instabilities in human cancers. *Nature*, **396**, 643–649.
18. Pihan, G. & Doxsey, S. J. (2003). Mutations and aneuploidy: co-conspirators in cancer? *Cancer Cell*, **4**, 89–94.
19. Dai, W., Wang, Q., Liu, T., Swamy, M., Fang, Y., Xie, S. *et al.* (2004). Slippage of mitotic arrest and enhanced tumor development in mice with BubR1 haploinsufficiency. *Cancer Res.* **15**, 440–445.
20. Dobles, M., Liberal, V., Scott, M., Benezra, R. & Sorger, P. K. (2000). Chromosome missegregation and apoptosis in mice lacking the mitotic checkpoint protein Mad2. *Cell*, **101**, 635–645.
21. Michel, L., Liberal, V., Chatterjee, A., Kirchwegger, R., Pasche, B., Gerald, W. *et al.* (2001). MAD2 haploinsufficiency causes premature anapahase and chromosome instability in mammalian cells. *Nature*, **409**, 355–359.
22. Shin, H. J., Baek, K. H., Jeon, A. H., Park, M. T., Lee, S. J., Kang, C. M. *et al.* (2003). Dual roles of human BubR1, a mitotic checkpoint kinase, in the monitoring of chromosomal instability. *Cancer Cell*, **4**, 483–497.
23. Jin, D. Y., Spencer, F. & Jeang, K. T. (1998). Human T cell leukemia virus type 1 oncoprotein Tax targets the human mitotic checkpoint protein MAD1. *Cell*, **93**, 81–91.
24. Lavia, P., Mileo, A. M., Giordano, A. & Paggi, M. G. (2003). Emerging roles of DNA tumor viruses in cell proliferation: new insights into genomic instability. *Oncogene*, **22**, 6508–6516.
25. Forgues, M., Difilippantonio, M. J., Linke, S. P., Ried, T., Nagashima, K., Feden, J. *et al.* (2003). Involvement of Crm1 in hepatitis B virus X protein-induced aberrant centriole replication and abnormal mitotic spindles. *Mol. Cell. Biol.* **23**, 5282–5292.
26. Feitelson, M. A., Bun, B., Satiroglu Tufan, N. L., Liu, J., Pan, J. & Lian, Z. (2002). Genetic mechanisms of hepatocarcinogenesis. *Oncogene*, **21**, 2593–2604.
27. Maggioni, M., Coggi, G., Cassani, B., Bianchi, P., Romagnoli, S., Mandelli, A. *et al.* (2000). Molecular changes in hepatocellular dysplastic nodules on microdissected liver biopsies. *Hepatology*, **32**, 942–946.
28. Aizaki, H., Harada, T., Otsuka, M., Seki, N., Matsuda, M., Li, Y. W. *et al.* (2002). Expression profiling of liver cell lines expressing entire or parts of hepatitis C virus open reading frame. *Hepatology*, **36**, 1431–1438.
29. Arima, N., Kao, C. Y., Licht, T., Padmanabhan, R., Sasaguri, Y. & Padmanabhan, R. (2001). Modulation of cell growth by the hepatitis C virus non-structural protein NS5A. *J. Biol. Chem.* **276**, 12675–12684.
30. Meraldi, P., Honda, R. & Nigg, E. A. (2002). Aurora-A overexpression reveals tetraploidization as major route to centrosome amplification in $p53^{-/-}$ cells. *EMBO J.* **21**, 483–492.
31. Fujiwara, T., Bandi, M., Nitta, M., Ivanova, E. V., Bronson, R. T. & Pellman, D. (2005). Cytokinesis failure generating tetraploids promotes tumorigenesis in p53-null cells. *Nature*, **437**, 1043–1047.
32. Gorbsky, G. J. (1997). Cell cycle checkpoints: arresting progress in mitosis. *BioEssays*, **19**, 193–197.
33. den Elzen, N. & Pines, J. (2001). Cyclin A is destroyed in prometaphase and can delay chromosome alignment and anaphase. *J. Cell Biol.* **146**, 1021–1032.
34. Geley, S., Kramer, E., Gieffers, C., Gannon, J., Peters, J. M. & Hunt, T. (2001). Anaphase-promoting complex/cyclosome-dependent proteolysis of human cyclin A starts at the beginning of mitosis and is not subject to the spindle assembly checkpoint. *J. Cell Biol.* **153**, 137–148.
35. Taylor, S. S., Ha, E. & McKeon, F. (1998). The human homologue of Bub3 is required for kinetochore localization of Bub1 and a Mad3/Bub1-related protein kinase. *J. Cell Biol.* **142**, 1–11.
36. Cahill, D. P., Lengauer, C., Yu, J., Riggins, G. J., Willson, J. K., Markowitz, S. D. *et al.* (1998). Mutations of mitotic checkpoint genes in human cancers. *Nature*, **392**, 300–303.
37. Minn, A. J., Boise, L. H. & Thompson, C. B. (1996). Expression of Bcl-xL and loss of p53 can cooperate to overcome a cell cycle checkpoint induced by mitotic spindle damage. *Genes Dev.* **10**, 2621–2631.
38. Taylor, S. S. & McKeon, F. (1997). Kinetochore localization of murine Bub1 is required for normal mitotic timing and checkpoint response to spindle damage. *Cell*, **89**, 727–735.

39. Albertson, D. G. & Pinkel, D. (2003). Genomic microarrays in human genetic disease and cancer. *Hum. Mol. Genet.* **12**, R145–R152.
40. Hwang, L. H., Lau, L. F., Smith, D. L., Mistrot, C. A., Hardwick, K. G., Hwang, E. S. *et al.* (1998). Budding yeast Cdc20: a target of the spindle checkpoint. *Science*, **279**, 1041–1044.
41. Gong, G., Waris, G., Tanveer, R. & Siddiqui, A. (2001). Human hepatitis C virus NS5A protein alters intracellular calcium levels, induces oxidative stress, and activates STAT-3 and NF-kappa B. *Proc. Natl Acad. Sci. USA*, **98**, 9599–9604.
42. Tai, D. I., Tsai, S. L., Chen, Y. M., Chuang, Y. L., Peng, C. Y., Sheen, I. S. *et al.* (2000). Activation of nuclear factor kappaB in hepatitis C virus infection: implications for pathogenesis and hepatocarcinogenesis. *Hepatology*, **31**, 656–664.
43. Mercurio, F. & Manning, A. M. (1999). NF-kappaB as a primary regulator of the stress response. *Oncogene*, **18**, 6163–6171.
44. Hayashi, J., Aoki, H., Arakawa, Y. & Hino, O. (1999). Hepatitis C virus and hepatocarcinogenesis. *Intervirology*, **42**, 205–210.
45. Idilman, R., De Maria, N., Colantoni, A. & Van Thiel, D. H. (1998). Pathogenesis of hepatitis B and C-induced hepatocellular carcinoma. *J. Viral Hepat.* **5**, 285–299.
46. Teramoto, T., Satonaka, K., Kitazawa, S., Fujimori, T., Hayashi, K. & Maeda, S. (1994). p53 gene abnormalities are closely related to hepatoviral infections and occur at a late stage of hepatocarcinogenesis. *Cancer Res.* **54**, 231–235.
47. Andreassen, P. R., Lohez, O. D., Lacroix, F. B. & Margolis, R. L. (2001). Tetraploid state induces p53-dependent arrest of nontransformed mammalian cells in G1. *Mol. Biol. Cell*, **12**, 1315–1328.
48. Zhou, H., Kuang, J., Zhong, L., Kuo, W. L., Gray, J. W., Sahin, A. *et al.* (1998). Tumour amplified kinase STK15/BTAK induces centrosome amplification, aneuploidy and transformation. *Nature Genet.* **20**, 189–193.
49. Jiang, Y., Zhang, Y., Lees, E. & Seghezzi, W. (2003). Aurora A overexpression overrides the mitotic spindle checkpoint triggered by nocodazole, a microtubule destabilizer. *Oncogene*, **22**, 8293–8301.
50. Shimakami, T., Hijikata, M., Luo, H., Ma, Y. Y., Kaneko, S., Shimotohno, K. & Murakami, S. (2004). Effect of interaction between hepatitis C virus NS5A and NS5B on hepatitis C virus RNA replication with the hepatitis C virus replicon. *J. Virol.* **78**, 2738–2748.
51. Shirota, Y., Luo, H., Qin, W., Kaneko, S., Yamashita, T., Kobayashi, K. & Murakami, S. (2002). Hepatitis C virus (HCV) NS5A binds RNA-dependent RNA polymerase (RdRP) NS5B and modulates RNA-dependent RNA polymerase activity. *J. Biol. Chem.* **277**, 11149–11155.
52. Lee, C. W., Sorensen, T. S., Shikama, N. & La Thangue, N. B. (1998). Functional interplay between p53 and E2F through co-activator p300. *Oncogene*, **16**, 2695–2710.

Edited by J. Karn

(Received 17 October 2005; received in revised form 3 March 2006; accepted 9 March 2006)
Available online 29 March 2006

PO Box 2345, Beijing 100023, China
www.wjgnet.com
wjg@wjgnet.com

World J Gastroenterol 2006 March 28; 12(12): 1881-1888
World Journal of Gastroenterology ISSN 1007-9327

BASIC RESEARCH

Reconstruction of liver organoid using a bioreactor

Masaya Saito, Tomokazu Matsuura, Takahiro Masaki, Haruka Maehashi, Keiko Shimizu, Yoshiaki Hataba, Tohru Iwahori, Tetsuro Suzuki, Filip Braet

Masaya Saito, Division of Gastroenterology and Hepatology, Department of Internal Medicine, The Jikei University School of Medicine, Tokyo, Japan
Tomokazu Matsuura, Department of Laboratory Medicine, The Jikei University School of Medicine, Tokyo, Japan
Takahiro Masaki, Tetsuro Suzuki, Department of Virology II, National Institute of Infectious Disease, Tokyo, Japan
Haruka Maehashi, Keiko Shimizu, First Department of Biochemistry, The Jikei University School of Medicine, Tokyo, Japan
Yoshiaki Hataba, DNA Medical Institute, The Jikei University School of Medicine, Tokyo, Japan
Tohru Iwahori, Fifth Division of Blood Purification, Department of Surgery, Tokyo Medical University, Tokyo, Japan
Filip Braet, Australian Key Center for Microscopy & Microanalysis, Electron Microscope Unit, The University of Sydney, NSW 2006, Australia
Supported by grants-in-aid from the University Start-Up Creation Support System, the Promotion and Mutual Aid Corporation for Private Schools of Japan, and The Japan Health Sciences Foundation (Research on Health Sciences on Drug Innovation, KH71068)
Correspondence to: Tomokazu Matsuura, MD, PhD, Department of Laboratory Medicine, The Jikei University School of Medicine, 3-25-8 Nishi-shinbashi, Minato-ku, Tokyo 105-8461, Japan. matsuurat@jikei.ac.jp
Telephone: +81-3-34331111-3210 Fax: +81-3-34350569
Received: 2005-09-12 Accepted: 2005-10-26

Abstract

AIM: To develop the effective technology for reconstruction of a liver organ *in vitro* using a bio-artificial liver.

METHODS: We previously reported that a radial-flow bioreactor (RFB) could provide a three-dimensional high-density culture system. We presently reconstructed the liver organoid using a functional human hepatocellular carcinoma cell line (FLC-5) as hepatocytes together with mouse immortalized sinusoidal endothelial cell (SEC) line M1 and mouse immortalized hepatic stellate cell (HSC) line A7 as non parenchymal cells in the RFB. Two x 10^7 FLC-5 cells were incubated in the RFB. After 5 d, 2 x 10^7 A7 cells were added in a similar manner followed by another addition of 10^7 M1 cells 5 d later. After three days of perfusion, some cellulose beads with the adherent cells were harvested. The last incubation period included perfusion with 200 nmol/L swinholide A for 2 h and then the remaining cellulose beads along with adherent cells were harvested from the RFB. The cell morphology was observed by transmission electron microscopy (TEM) and scanning electron microscopy (SEM). To assess hepatocyte function, we compared mRNA expression for urea cycle enzymes as well as albumin synthesis by FLC-5 in monolayer cultures compared to those of single-type cultures and cocultures in the RFB.

RESULTS: By transmission electron microscopy, FLC-5, M1, and A7 were arranged in relation to the perfusion side in a liver-like organization. Structures resembling bile canaliculi were seen between FCL-5 cells. Scanning electron microscopy demonstrated fenestrae on SEC surfaces. The number of vesiculo-vacuolar organelles (VVO) and fenestrae increased when we introduced the actin-binding agent swinholide-A in the RFB for 2h. With respect to liver function, urea was found in the medium, and expression of mRNAs encoding arginosuccinate synthetase and arginase increased when the three cell types were cocultured in the RFB. However, albumin synthesis decreased.

CONCLUSION: Co-culture in the RFB system can dramatically change the structure and function of all cell types, including the functional characteristics of hepatocytes. Our system proves effective for reconstruction of a liver organoid using a bio-artificial liver.

Key words: Liver organoid; Organ reconstruction; Bio-artificial liver; Coculture; Liver sinusoidal endothelial cell; Hepatocytes; Fenestrae; Vesiculo vacuolar organelles; Radial flow bioreactor

Saito M, Matsuura T, Masaki T, Maehashi H, Shimizu K, Hataba Y, Iwahori T, Suzuki T, Braet F. Reconstruction of liver organoid using a bioreactor. *World J Gastroenterol* 2006; 12(12): 1881-1888

http://www.wjgnet.com/1007-9327/12/1881.asp

INTRODUCTION

Liver regeneration technology has made many advances in recent years. Efforts now are being made toward development of embryonic stem cells (ES cells), differentiation of hemopoietic stem cells, and development of isolation and culture methods for somatic stem cells originating from different organs. Hemopoietic stem cells, hepatoblasts originating from fetal liver, hepatocytes, and pancreatic duct epithelial cells have been included in the list of candi-

date cells for liver regeneration[11]. Development of immortalized cells by introduction of the simian virus 40 (SV40) large T antigen gene or human telomerase reverse transcriptase (hTERT) is also under investigation[12]. To date, however, no technique for regenerating and reconstructing parenchymal organs using these cells has been established. Conventional cell culture methods have achieved this goal clinically for skin, cornea, and bone tissue[13-15].

Reconstruction of organs such as the liver requires maintenance of viable cells at a high density and coculture under conditions favorable to several different cell types that constitute a liver. To make a culture system is important in reconstructing a liver organoid. Conventional stationary culture techniques are not well suited to the culture of cells in a layered form, i.e., in a structural and functional organoid a simple air/CO_2 incubator does not deliver adequate oxygen supply to layered cells. Furthermore, high-density culture cannot be maintained with the limited nutrients available in conventional cultures. For these reasons, construction of a bioreactor that allows 3-dimensional growth in a high-density perfusion culture has been advocated for reconstructing a liver organoid. In our study a radial-flow bioreactor (RFB) developed in Japan was used as a candidate model for high-density perfusion culture. Filled with a porous carrier, this bioreactor permits culture at a cell density 10 times higher than that allowed by a hollow-fiber culture system[16-17]. Another important point is to select a cell source. Clinically, cells using bio-artificial liver are required to be highly functional and supplied quickly in large quantities. Therefore we established a functional human hepatocellular carcinoma cell line (FLC-5), which can express drug-metabolized enzymes (e.g., human-type carboxyl esterase or cytochrome) and liver-specific proteins such as albumin. *In vitro* this cell line retains its three-dimensional form, developing distinct microvilli on the surface. These cells can be cultured in serum-free ASF104 medium (Ajinomoto, Tokyo). A liver organoid cannot be reconstructed with hepatocytes only. At minimum, coculture of hepatocytes with nonparenchymal cells, such as sinusoidal endothelial cell (SEC) and hepatic stellate cell (HSC) is required. So we established immortalized SEC line M1[18] and an immortalized HSC line A^{-}[19] by isolating nonparenchymal cells from an H-2Kb-tsA58-transgenic mouse liver transfected with the SV40 large T antigen gene[10].

Reconstruction of the liver sinusoid is important for activity of the liver organoid as a functional unit. Also, the open pores on the surfaces of SEC in fenestrae have an important functional role in the liver sinusoid. Fenestrae are the most remarkable characteristics of SEC, as first described by Wisse in 1970[20] using transmission electron microscopy (TEM). Diameters of these pores vary between species, ranging from 100 to 200 nm[21]. These fenestrae facilitate the transport of materials and solutes from the luminal to the abluminal side of the liver parenchymal cells and *vice versa*[22]. The process and mechanism of formation of these pores remain largely unclarified[23,24]. The presence of actin filaments at the margin of these pores has been demonstrated by electron microscopic studies[25-27]. Swinholide A, a most potent microfilament-disrupting drug available, has been demonstrated to increase the number of SEC fenestrae[24]. However, when immortalized SEC was treated in a monolayer culture or as a monoculture in the RFB, an increase in number of fenestrae could not be observed when the Swinholide A was introduced. The potential for drug-induced increase also has been reported to disappear in long-term cultures[28].

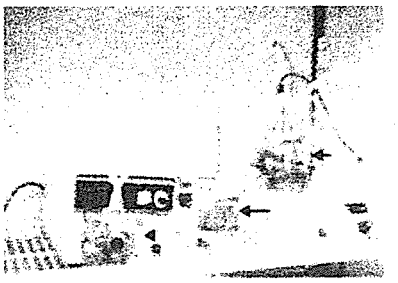

Figure 1 The system of radial-flow bioreactor. A 15-mL radial-flow bioreactor (large arrow), a mass flow controller (arrow head), and a reservoir (small arrow) are connected each other. Culture medium is perfused in the RFB. Medium conditions (PH, oxygen, CO_2 and temperature) are controlled by computer.

In developing a high functioning organoid using a bio-artificial liver, the function, form and reactivity of pharmacological agent should be near *in vivo*. In the present study, we reconstructed a functional liver organoid using immortalized cell lines in the RFB.

MATERIALS AND METHODS

Cell culture and medium

We used the three cell lines mentioned above, FLC-5, M1, and A^{-}. As reported, culture of M1 cells was possible in serum-free conditions while supplementation of ASF104 medium with 2% fetal bovine serum (FBS) was required for culture of A^{-} cells. Therefore, in coculture experiments, ASF104 medium was enriched with 2% FBS.

Coculture in radial-flow bioreactor

As reported elsewhere, the RFB system is composed of a 15-mL radial-flow chamber (RA-15; ABLE, Tokyo), a mass flow controller (RAD925, ABLE), a reservoir (Figure 1), a computer, and a tissue incubator as described previously[16] (Figure 1). The culture medium was oxygenated within the reservoir, and the pH was adjusted automatically to 7.4. Oxygen pressure in the culture medium was measured both within the reservoir and at the outlet of the bioreactor. Relative oxygen consumption was monitored on the basis of the oxygen pressure gradient. During the study the temperature within the reservoir was kept constantly at 37 ℃. Two × 10^{7} FLC-5 cells were inoculated into the reservoir. The bioreactor was perfused in a closed circuit for 2 h to aid cells in adhering to the porous carrier cellulose beads (Asahi Kasei, Tokyo). Subsequently the bioreactor was switched to the open-circuit mode, and incubation was continued with addition of fresh culture medium to the reservoir. After 5 d, 2 × 10^{7} A^{-} cells were added in a similar manner followed by another addition of 10^{7} M1 cells 5 d later. Retinol (10^{-6} mol/L) was added during the first 2 d. After three days of perfusion cellulose beads with the adherent cells were harvested, and cells deposited at the bottom of the bioreactor also were recovered. Beads with attached cells were fixed in 1.2% or 2.0% glutaraldehyde as described below.

Swinholide A experiments

We cultured the three cell lines as described above. The

last incubation included perfusion with 200 nmol/L swinholide A (Sigma catalog number S9810; S) for 2 h. The cellulose beads along with adherent cells were harvested from the bioreactor. Beads with attached cells were fixed in glutaraldehyde and prepared for morphologic observation as follows.

Electron microscopy

For scanning electron microscopy (SEM), cultured cells were fixed with 1.2% glutaraldehyde in 0.1 mol/L phosphate buffer (PB) at pH 7.4 and postfixed with 1% OsO_4 in 0.1mol/L PB. The fixed cells were rinsed twice with PBS, subsequently dehydrated in ascending concentrations of ethanol, critical point-dried using carbon dioxide, and coated by vacuum- evaporated carbon and ion-spattered gold. Specimens were observed under JSM-35 scanning electron microscope (JEOL, Tokyo) at an accelerated voltage of 10 kV.

For transmission electron microscopy (TEM), cultured cells were fixed with 2.0% glutaraldehyde in 0.1mol/L PB for 1 h and postfixed with 1% OsO_4 in 0.1mol/L PB for 1 h at 4 ℃. Specimens were dehydrated in ethanol and subsequently embedded in a mixture of Epon-Araldite. Thin sections (60 nm) were cut with a diamond knife mounted on an LKB ultratome, and stained with aqueous uranyl acetate. Specimens were examined under a JEOL 1200EX electron microscope.

Amino acid analysis of supernatants

For analysis of amino acid fractions by high-performance liquid chromatography (HPLC), supernatants were collected from FLC-5 alone and from cocultures of the three cell types in the bioreactor. Supernatants were mixed with 5% sulfosalicylic acid and allowed to stand at 4 ℃ for 15 min. After centrifugation to precipitate protein, supernatants were injected into amino acid analysis columns (L-8500, Hitachi, Tokyo).

Quantitative TaqMan RT-PCR

We measured mRNA expression for the urea cycle enzymes, carbamoyl phosphate synthetase (CPS1), ornithine carbamoyltransferase (OCT), argininosuccinatesynthetase (ASS), argininosuccinatelyase (ASL), and arginase (ARG), as well as mRNA expression for albumin, hepatocyte nuclear factor (HNF)-1 and HNF-4, by quantitative TaqMan reverse transcription polymerase chain reaction (RT-PCR). RT-PCR was performed on the ABI PRISM ⁻⁻00 sequence detection system using random hexamers from TaqMan reverse transcription reagents and the RT reaction mix (Applied Biosystems, Rockville, M) to reverse-transcribe RNA. TaqMan universal PCR Master Mix and Assays-on-Demand gene expression probes (Applied Biosystems) were used for PCR. A standard curve for serial dilution of 18S rRNAs was generated similarly. A relative standard curve method (Applied Biosystems) was used to calculate the amplification difference in urea cycle-related enzymes between cocultured and control cells, and elongation factor 1 (EF1), for each primer set and between albumin, HNF-1, HNF-4, and glyceraldehyde-3-phosphate dehydrogenase (GAPDH). Specificity was evaluated using GAPDH mRNA as an internal control (4310884E; Perkin-Elmer Applied Biosystems). Each amplification was performed in triplicate, and averages were obtained.

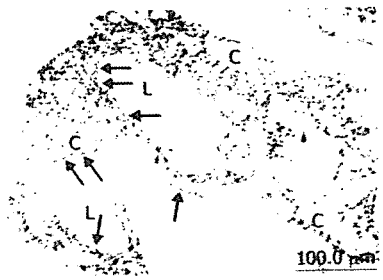

Figure 2 Light microscopic image of coculture in the RFB. High-density and layered cells attached on the cellulose beads (C). Sinusoid-like lumen structure (L) could be observed. SEC was observed with flat shape on surface of the lumen and perfusion side (arrow).

Based on DNA sequences in GenBank, primers and the TaqMan probe for albumin, HNF-1, and HNF-4 were designed using the primer design software Primer Express TM (Perkin-Elmer Applied Biosystems, Foster City, CA). AmpliTaq DNA polymerase extended the primer and displaced the TaqMan probe through its 5'-3' exonuclease activity. Probes were labeled with a reporter fluorescent dye either 6-carboxy-fluorescein (FAM) or 2, ⁻ dimethoxy-4,5-dichloro-6-carboxy-fluorescein (JOE) at the 5' end and a quencher fluorescent dye [6-carboxytetramethyl-rhodamine (TAMRA)] at the 3' end.

Primers/probes were as follows: ornithine transcarbamoylase (OTC) forward primer 5'-CCAGGCAATA-AAAGAGTCAGGATT-3', reverse primer/ 5'-TTAT-CAAAG TCCCCTGGTTAGAGATACT-3', probe/ 5' -(FAM)- TTCAAATGCTCCTACACCCTGCCCTG-(TAMRA)-3'; arginosuccinase (ASL) forward primer/ 5' -TGGCCAAGGAGGTCGTCA-3', reverse primer 5' -TTCCTCGTCGTCCGGAAG-3', probe 5'-(FAM)-TGTCTTCCAGACCCGGAGACCGAA-(TAMRA)-3'; albumin forward primer/ 5'-CGATTTTCTTTT-TAGGGCAGTAGC-3', reverse primer/ 5'-TG-GAAACTTCTGCAAACTCAGC-3', probe/ 5'-(FAM)-CGCCTGAGCCAGAGATTTCCCA-(TAMRA)-3'; HNF-1 forward primer/ 5'-AGCGGGAGGTGGTC-GATAC-3', reverse primer/ 5'-CATGGGAGTGCCCTT-GTTG-3', probe/ 5'-(FAM)-TCAACCAGTCCCACCT-GTCCCAACA-(TAMRA)-3'; HNF-4 forward primer/ 5'-GGTGTCCATACGCATCCTTGA-3', reverse primer/ 5'-TGGCTTTGAGGTAGGCATACTCA-3', probe/ 5'-(FAM)-CCTTCCAGGAGCTGCAGATC-GATGAC-(TAMRA)-3'; GAPDH forward primer/ 5' -CTCCCCACACACATGCACTTA-3', reverse primer/ 5' -CCTAGTCCCAGGGCTTTGATT-3', probe/ 5'-(VIC)-AAAAGAGCTAGGAAGGACAGGCAACTTGGC-(TAMRA)-3'.

RESULTS

Structure of cells cultured in bioreactor

In the bioreactor, cells cultured in high density assumed layered form on the cellulose beads. Lumen-like structure was observed. Endothelial cells were exits with flat shape at the surface of the lumen and the perfusion side (Figure 2). Multiple layers of FLC-5 cells adhered to the cellulose beads, while A⁻ and M1 cells were predominantly localized to the side where perfusion occurred. Layered cells were seen in a hole of porous cellulose beads. Sinusoid-like lumen was observed at perfusion side in the cellulose beads